ISTANBUL TECHNICAL UNIVERSITY ★ GRADUATE SCHOOL OF SCIENCE ENGINEERING AND TECHNOLOGY

CONTRIBUTIONS TO ANALYSIS OF EFFECT OF WINDING GEOMETRY ON FORCES AND MECHANICAL DEFORMATIONS ON DISTRIBUTION TRANSFORMERS WINDINGS CAUSED UNDER SHORT-CIRCUIT OPERATION

M.Sc. THESIS

Sadulah KAYA

Department of Electrical Engineering

Electrical Engineering Programme

MAY 2015

ISTANBUL TECHNICAL UNIVERSITY ★ GRADUATE SCHOOL OF SCIENCE ENGINEERING AND TECHNOLOGY

CONTRIBUTIONS TO ANALYSIS OF EFFECT OF WINDING GEOMETRY ON FORCES AND MECHANICAL DEFORMATIONS ON DISTRIBUTION TRANSFORMERS WINDINGS CAUSED UNDER SHORT-CIRCUIT OPERATION

M.Sc. THESIS

Sadulah KAYA
(504101059)

Department of Electrical Engineering

Electrical Engineering Programme

Thesis Advisor: Asst. Prof. Dr. Derya Ahmet KOCABAŞ

04 MAY 2015

İSTANBUL TEKNİK ÜNİVERSİTESİ ★ FEN BİLİMLERİ ENSTİTÜSÜ

SARGI GEOMETRİSİNİN KISA DEVRE DURUMUNDA DAĞITIM TRANSFORMATÖRLERİ SARGI KUVVETLERİ VE MEKANİK DEFORMASYONLARINA ETKİSİNİN İNCELENMESİNE KATKILAR

YÜKSEK LİSANS TEZİ

Sadulah KAYA
(504101059)

Elektrik Mühendisliği Anabilim Dalı

Elektrik Mühendisliği Programı

Tez Danışmanı: Yrd. Doç. Dr. Derya Ahmet KOCABAŞ

04 MAYIS 2015

Sadulah KAYA, a **M.Sc.** student of **ITU Graduate School of Science Engineering and Technology** student ID 504101059, successfully defended the thesis entitled "**CONTRIBUTIONS TO ANALYSIS OF EFFECT OF WINDING GEOMETRY ON FORCES AND MECHANICAL DEFORMATIONS ON DISTRIBUTION TRANSFORMERS WINDINGS CAUSED UNDER SHORT-CIRCUIT OPERATION**", which he prepared after fulfilling the requirements specified in the associated legislations, before the jury whose signatures are below.

Thesis Advisor : **Asst. Prof. Dr. Derya Ahmet KOCABAŞ**
İstanbul Technical University

Jury Members : **Asst. Prof. Dr. Derya Ahmet KOCABAŞ**
İstanbul Technical University

Assc. Prof. Dr. Güven KÖMÜRGÖZ KIRIŞ
İstanbul Technical University

Prof. Dr. İbrahim ŞENOL
Yıldız Technical University

Date of Submission : 04 May 2015
Date of Defense : 28 May 2015

FOREWORD

I would like to thank my thesis supervisor, Asst. Prof. Dr. Derya Ahmet KOCABAŞ, for his guidance and support. I would also like to thank Lecturer Emin SÜNBÜLOĞLU (Phd.) and Res. Asst. M. Onur Gülbahçe (MSc.) for answering my questions during my study.

May 2015

Sadulah KAYA
Electrical and Electronics Engineer

TABLE OF CONTENTS

Page

ABBREVIATIONS

IEC **:** International Electrotechnical Commission
Uk **:** Short Circuit Impedance
ONAN **:** Oil Natural Air Natural
LV **:** Low Voltage
HV **:** High Voltage

LIST OF TABLES

Page

LIST OF FIGURES

Page

CONTRIBUTIONS TO ANALYSIS OF EFFECT OF WINDING GEOMETRY ON FORCES AND MECHANICAL DEFORMATIONS ON DISTRIBUTION TRANSFORMERS WINDINGS CAUSED UNDER SHORT-CIRCUIT OPERATION

SUMMARY

Electrical power systems are mainly composed of generation, transmission and distribution circuits operating at different voltage levels. Interface between these circuits is provided by transformers, which are expensive, heavy and hard to install. Additionally, purchasing period for transformers is relatively long. These facts make transformers have to be robust enough and withstand stresses during operation for reliability of entire power system.

Current passing through transformer windings causes electromagnetic forces, which are proportional to the square of current. During short circuit between transformer and load, peak current value becomes 28-70 times the nominal current depending on system and transformer short circuit impedance. Extreme forces on transformer windings may cause damages although circuit breakers interrupt current in a short time period. The forces on windings also depend on the time instant when the short circuit takes place. However, the case that causes maximum force should be simulated to ensure the transformer withstands forces. It is known that irreversible deformations and displacements will reduce the durability of the transformer for the next short-circuit operation.

In this thesis, different transformer winding designs under same design constraints are compared in terms of forces created during worst-case short-circuit operation and mechanical displacements and deformations in winding structures are obtained. Results are given in comparison.

A transformer with specified technical characteristics can be designed in several ways. Changing winding geometry is one of the alternatives for design. In this study, a three-phase power transformer with same power, voltage, frequency, loss values is designed in three different winding geometries namely cylindrical, elliptical and square. Design constraints like flux density, copper current density, core loss factor etc. are also kept unchanged for three designs. Under these design constraints, for each design, worst-case analysis is performed under short circuit conditions. Forces are obtained by calculation and electromagnetic simulation software, Maxwell. Force distribution is almost uniform on cylindrical design while it differs in different regions of elliptical and square windings. Force on narrow part of elliptical windings is less than the wide part, which is sharper. Similarly, forces obtained for flat parts of square design are less than those obtained for corner parts are. Additionally, it is observed that maximum forces on cylindrical windings are less than maximum forces on elliptical and square windings. Square windings are subjected to the highest forces among three types of transformers under short circuit conditions.

The forces obtained by electromagnetic simulation software are maximum instantaneous forces affecting the windings under worst-case short circuit. These forces decrease in time and take their continuous form in time depending on the current waveforms depending on the system and transformer parameters. Transformer parameters for three designs are calculated and force variations on windings are obtained.

ANSYS software is utilized in order to simulate the mechanical deformation and stress on transformer windings under short circuit. Transformer structures are simplified and forces are applied to the simplified structures. Obtaining the results, it is observed that deformation and stress on cylindrical design is minimum while the deformation and stress on square design is maximum among three designs.

SARGI GEOMETRİSİNİN KISA DEVRE DURUMUNDA DAĞITIM TRANSFORMATÖRLERİ SARGI KUVVETLERİ VE MEKANİK DEFORMASYONLARINA ETKİSİNİN İNCELENMESİNE KATKILAR

ÖZET

Elektrik enerji sistemleri temel olarak farklı gerilim seviyelerinde çalışan üretim, iletim ve dağıtım alt sistemlerinden oluşur. Farklı gerilim seviyelerinde çalışan alt sistemlerin birbirleriyle bağlantısı transformatörler aracılığıyla sağlanır. Transformatörler pahalı ve ağır ekipmanlar olup ciddi bir arıza durumunda arızalı transformatörün demontajı ve tamiri görece zordur. Arızası giderilmiş ya da temin edilmiş transformatörün montajı da aynı şekilde enerji sisteminin diğer ekipmanlarına göre zaman alıcı ve zordur. Ayrıca transformatörlerin temin edilmesi çoğu zaman uzun süreler gerektirmektedir. Bu sebeplerden dolayı tüm enerji sisteminin güvenilirliği açısından transformatörlerin çalışma esnasında karşılaşılacak zorlamalara karşı dayanıklı olmaları beklenmektedir.

Transformatör sargıları akım iletirken manyetik alan oluştururlar. Sargılar aynı zamanda manyetik alan bulunan ortamda akım taşıdıklarından çekme veya itme kuvvetlerine maruz kalırlar. Bu kuvvetler transformatör akımının karesiyle orantılıdır. Kısa devre durumunda transformatör ve sistem eşdeğer empedansına bağlı olarak transformatör akımı tepe değeri nominal akımın 28-70 katına çıkabilmektedir. Ayrıca kısa devrenin oluştuğu an da kısa devre ani akımının büyüklüğünde etkilidir. Kısa devre durumda kesicilerin akımı kısa sürede kesmesine rağmen transformatör sargıları çok büyük kuvvetlere maruz kaldığından transformatörlerde deformasyonlar oluşabilmektedir. Geri dönüşü olmayan yer değiştirme ve deformasyonların, transformatörün ilerleyen süreçte karşılaşacağı olası kısa devre durumları karşısında dayanımını düşüreceği açıktır. Bu nedenle transformatörün kısa devrelere dayandığından emin olunması amacıyla transformatörü en çok zorlayacak kısa devre durumu için kuvvet hesaplamalarının yapılması ve bu kuvvetlerin transformatöre etkilerinin incelenmesi önem arz etmektedir. Bu çalışmada sargı geometrisinin kısa devre durumunda transformatör sargılarında oluşacak kuvvetlere ve bu kuvvetlerin neden olacağı yer değiştirme ve deformasyonlara etkisinin gösterilmesi amaçlanmaktadır.

Teknik karakteristikleri belirli bir transformatörün tasarımı birden fazla şekilde yapılabilir. Transformatör sargılarının geometrisinin değiştirilmesi, aynı teknik özelliklerde değişik transformatör tasarımları elde etmek için izlenebilecek yollardan biridir. Bu çalışmada aynı güç, gerilim, kayıp, frekans, kısa devre gerilimi vb. teknik özelliklere sahip üç fazlı üç farklı transformatörün tasarımı, sargı geometrileri silindirik, eliptik ve kare olmak üzere yapılmıştır. Bu tasarımlar esnasında akı yoğunluğu, bakır akım yoğunluğu, çekirdek kayıp faktörü vb. teknik parametreler üç tasarım için aynı alınmıştır. Tasarımın tamamlanmasının ardından her bir tasarım için en zorlayıcı kısa devre durumu benzetimi yapılmıştır.

Sistem çalışma gerilimi sabit alınmak kaydıyla kısa devre akımı transformatör ve diğer sistem elemanlarının eşdeğer empedansına ve ayrıca kısa devrenin oluştuğu zamana bağlıdır. Anlık akım değeri, kısa devrenin oluşma zamanına göre nominal kısa devre akımının yaklaşık iki katına kadar çıkabilmektedir. Bu akım, eşdeğer direnç ve endüktans değerlerinin oranına bağlı olarak zamanla azalmakta ve nominal değerine ulaşmaktadır. Transformatörlerin kısa devre durumu benzetimi yapılırken sistemin transformatör haricindeki eşdeğer empedansı sıfır olarak alınmış ve en zorlayıcı durumu oluşturacak anda kısa devre gerçekleştiği farz edilip hesaplamalar yapılmıştır.

Kısa devre durumunda sargılar üzerinde oluşan kuvvetlerin büyüklüğü hesaplama yöntemiyle elde edilebilmektedir. Kuvvetlerin sargılar üzerinde dağılımının elde edilmesi için ilave yöntemlere ihtiyaç vardır. Bu dağılımlar elektromanyetik analiz programları vasıtasıyla elde edilmiştir. Silindirik sargılı transformatör için hesapla elde edilen sonuçla analiz sonuçları karşılaştırılmıştır. Değerlerin birbirine yakın olduğu tespit edildikten sonra üç tasarım için sargılar üzerindeki kuvvetlerin büyüklüğü ve dağılımı elektromanyetik analiz yazılımı Maxwell ile elde edilmiştir. Silindirik sargılı transformatörde sargılar üzerindeki kuvvetler sargılar boyunca eşit dağılmaktadır. Eliptik ve kare sargılı transformatörlerde ise bu durum farklılık göstermektedir. Eliptik sargılı transformatörde elipsin sivri uçlarındaki akı yoğunluğu daha düz olan kısımlardaki akı yoğunluğundan yüksektir. Benzer şekilde kare sargılı transformatörde sargı köşelerindeki akı yoğunluğu düz olan kısımlara göre daha yüksektir. Bu durumdan dolayı eliptik sargılı transformatörde sivri uçlardaki kuvvetlerin düz kısımlardaki kuvvetlere göre daha şiddetli olduğu, aynı şekilde kare sargılı transformatörün köşelerindeki kuvvetlerin de düz kısımdaki kuvvetlere göre daha şiddetli olduğu görülmektedir.

Aynı transformatörün sivri bölgelerinde daha fazla kuvvet oluşmasına benzer bir durum farklı tasarımların karşılaştırılmasında da gözlenmektedir. Silindirik sargılı transformatörde, sargılarda diğer tasarımlarda olduğu gibi sivri uç bulunmamasından dolayı kısa devre durumunda oluşan kuvvetler en düşük seviyededir. Eliptik sargılı transformatörde kısa devre durumunda oluşan elektromanyetik kuvvetler silindirik sargılı transformatör sargılarında oluşan kuvvetlere oranla daha şiddetlidir. En şiddetli kısa devre kuvvetleri ise kare sargılı transformatörün köşelerinde oluşmaktadır.

Farklı sargı geometrilerine sahip üç transformatörün sargılarında oluşan kısa devre kuvvetlerinin büyüklükleri ve kuvvetlerin sargılar üzerindeki dağılımları elde edildikten sonra bu kuvvetlerin transformatörlerde oluşturacağı yapısal etkilerin incelenmesi ve sonuçların karşılaştırılması istenmektedir. Bu amaçla her üç transformatör için daha önceden oluşturulan üç boyutlu çizimler üzerine elektromanyetik analiz programıyla elde edilmiş kuvvetler eşdeğer basınç değerlerine dönüştürülüp standartlarla belirlenen süre boyunca uygulanmıştır. Kısa devre durumu mekanik benzetimi için ANSYS yazılımı kullanılmıştır. Yazılımın çalıştırılması için öncelikle transformatörlerin imalatında kullanılan malzemeler tanımlanmış ve teknik özellikleri analize işlenmiştir. Analizdeki işlem sayısını azaltmak için transformatörlerin yapısındaki simetriden faydalanılarak analizde kullanılacak yapı basitleştirilmiştir.

En zorlayıcı kısa devre durumu analizi yapılacağı için yapılan varsayımlarla elde edilen kısa devre ilk akımı tepe değer olup bu akım zaman içinde azalmakta ve akımın eksponansiyel kısmı sıfırlanmaktadır. Transformatörlerin eşdeğer dirençleri ve endüktansları kullanılarak bulunan zaman sabitleriyle akımdaki azalma ve sinüsoidal devam etme durumu matematiksel ifade olarak elde edilmiştir. İlgili standartlarda belirtilen kısa devre test süresi 0,5 saniyedir. Her bir transformatör için bu süre zarfında akım değişimi elde edilmiş, transformatör sargılarındaki basınç değişiminin akımın karesinin zamanla değişimi oranında olacağından hareketle her bir transformatörün ilgili kısımları için zamanla değişen basınç elde edilmiştir.

Analiz 0-1 saniye arasında yapılmıştır. Standartlarda belirtilen kısa devre test süresi olan 0,5 saniyeden sonraki mekanik hareketlilik de bu sayede analiz kapsamına alınmıştır. Analiz sonuçlarına göre silindirik sargılardaki deformasyon diğer iki transformatörün sargılarındaki deformasyon değerlerinin çok altındadır. Eliptik sargılardaki deformasyon silindirik sargılardaki deformasyondan fazla olmakla beraber en yüksek deformasyon değerleri kare sargılı transformatörde alınmıştır. Üç farklı sargılı transformatör arasında silindirik sargılı transformatörün kısa devreden elektriksel ve mekanik olarak en az etkilendiği, kare sargılı transformatörün ise en fazla etkilendiği görülmüştür.

Sargılarda oluşan mekanik gerilim değerleri de deformasyonlarla paralellik göstermektedir. Silindirik sargılarda oluşan maksimum mekanik gerilimler diğer sargı tiplerinde oluşan gerilim değerlerinin çok altındadır. En fazla mekanik gerilimler kare sargılarda oluşmaktadır.

1. INTRODUCTION

Electrical power system is mainly composed of generation, transmission and distribution circuits operating at different voltage levels. A transformer is a static device that transfers electrical energy from one circuit to another by electromagnetic induction without the change in frequency [1].

For the reliability and continuity of a power system, like other components, transformers are supposed to withstand electrical, mechanical and thermal stresses during operation. High prices, long delivery dates, challenging transportation, loading, unloading and assembly processes are some reasons why users especially want the transformers to be robust enough and not to be defected once they are assembled.

1.1 Purpose of Thesis

A distribution or power transformer with specified technical characteristics (power, voltage, losses etc.) can be designed in more than one unique way. Changing the winding geometry is one of the alternatives for redesigning a transformer. Several kinds of transformers can be designed by changing the winding geometry with the same design procedure and materials. For each design, effect of electrical, mechanical and thermal stresses during operation should be simulated or calculated before manufacturing process begins to ensure the transformer can withstand those stresses.

Although different transformers with same technical specifications are formed with different geometries, stresses the transformers are subjected during normal operation, overloading and short circuit conditions are not same. In this study, it is aimed to show the effect of winding geometry on electromagnetic forces and the results of these forces on transformer structure under short-circuit conditions by calculating the forces, displacements and deformations on the windings since irreversible deformations and displacements will reduce the durability of the transformer for the next short-circuit operation. The results for three types of winding geometry, namely cylindrical, elliptical and square ones are obtained by calculations and simulations and are compared.

1.2 Literature Review

In order to see the effect of winding geometry on short circuit forces and deformation in transformers, transformer design should be performed first. In *Elektrik Makinaları Dersleri: Teori, Hesap, Konstrüksiyon cild.1* [2], theoretical background about transformers, operation principles, calculations related to transformer design and construction process for transformers are covered. *Transformers* [3] is one of the other books related to transformer design. Several more textbooks covering transformer design are available. Short circuit in electrical power systems is a significant phenomenon, which is covered by most of the power system textbooks. In *Power System Analysis* [4] and in *Electric Power Systems* [5], calculation of short circuit currents and variation of current in time are given in details. *Elektrik Makinalarında Aşırı Zorlanmalar* [6] is a textbook in which short circuit force calculations for transformers are covered. Additionally, in *Investigation of Transformer Electromagnetic Forces Caused by External Faults Using FEM* [7], the validity of FEM (Finite Element Method) for obtaining short circuit forces in transformers under external faults is checked by comparing the results with those obtained analytically. In *The Analysis of Mechanical Strength of HV Winding Using Finite Element Method, Part 1 Calculation of Electromagnetic Forces* [8], magnetic flux density and forces on transformer windings are obtained by finite element analysis software. Additionally, in *The Analysis of Mechanical Strength of HV Winding Using Finite Element Method, Part 2 Mechanical Stress and Deformation Analysis* [9], deformation and stress analysis of disks in the HV winding is performed using finite element method.

1.3 Hypothesis

Transformer low voltage and high voltage windings are composed of current carrying copper (or aluminum) coils. During normal operation of power system, these coils are subjected to radial and axial electromagnetic forces. Since the radial component of leakage flux is small enough for transformers having high voltage and low voltage windings with same height, axial forces are negligible [2]. Radial forces, which are inward for low voltage winding and outward for high voltage one, are proportional to the square of winding currents and these forces reach extreme level during short circuits in power system before the circuit breakers interrupt short circuit current to protect transformers and other components. Transformer coils are supposed to withstand these short circuit forces in that short period in order to operate normally after reenergizing the power system.

Short circuit forces acting on windings depend not only on the short circuit current but also on transformer design. Likewise, deformation on transformer after short circuit is correlated with design. A transformer with given technical characteristics can be designed in different geometries. Basically, cylindrical, elliptical and rectangular type of windings can be designed with same design constraints. Among these designs, force distributions on elliptical and rectangular windings are not uniform since windings face higher forces on sharper regions while those on cylindrical windings are close to uniform distribution. It is known that applying non-uniform force on structures, especially higher forces caused by sharp regions results with higher deformation on structure even if the forces are applied to a cylindrical shell. Moreover, even applying uniform force on elliptical or rectangular structures, the shells tend to get cylindrical because of the nature of materials. Using these two facts, cylindrical geometry is the one having minimum deformation after short circuit because of lower maximum force and the nature of structure itself.

Among three distribution transformers with same technical characteristics and unchanged design constraints, but with different winding geometries namely cylindrical, elliptical and square, it is expected that short circuit forces on cylindrical windings will be lowest. Additionally, deformations caused by short circuit forces are lowest for cylindrical design. Because of sharper regions on square windings, highest forces and deformations on windings under short circuit operation will occur in this type of windings.

2. TRANSFORMERS

A transformer is a static device that transfers electrical energy from one circuit to another by electromagnetic induction without the change in frequency. The transformer, which can link circuits with different voltages, has been instrumental in enabling universal use of the alternating current system for transmission and distribution of electrical energy. Various components of power system, viz. generators, transmission lines, distribution networks and finally the loads, can be operated at their most suited voltage levels. As the transmission voltages are increased to higher levels in some part of the power system, transformers again play a key role in interconnection of systems at different voltage levels. Transformers occupy prominent positions in the power system, being the vital links between generating stations and points of utilization [1].

The simplest transformer is a two winding construction consisting of three active elements: a closed iron core and two windings inductively coupled with the core. The windings of a two-winding transformer are distinguished either by their service condition or by their voltage levels. In terms of their service condition, the supplied winding is called the primary, and the loaded winding the secondary. In terms of their voltage levels, the terms high-voltage winding and low-voltage winding are used. Apart from a few very individual applications (generator-transformer, metallurgical furnace transformer etc.), either winding may act as primary or secondary depending on the system condition, whereas the roles of the high and low voltage windings obviously cannot be interchanged.

The principle of operation of the transformer can best be understood, to a first approximation, by considering the operation of a loss-free transformer. The loss-free transformer is one, which the resistance of the windings, and the hysteresis and eddy-current losses of the iron core, can be neglected. In the no load condition of such a transformer, i.e. when no loading impedance is connected across its secondary terminals, there is only a magnetic flux in the iron core (of peak value of ϕ) and all turns (N_1 and N_2) of the primary and secondary windings are linked with that flux. In this ideal case (figure 2.1 [10]) the instantaneous value of primary voltage is

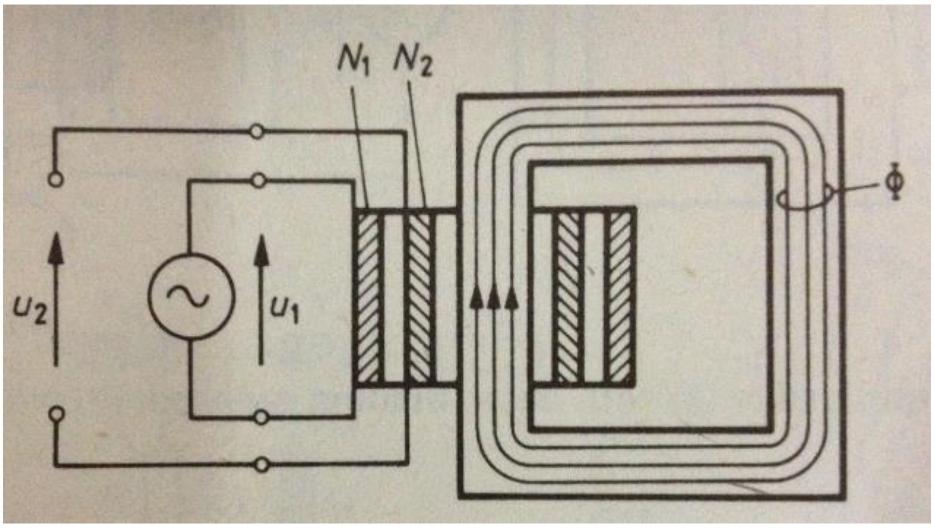

Figure 2.1 : Transformer under no-load condition.

$$u_1 = N_1 \frac{d\varphi}{dt} \quad \textbf{(2.1)}$$

and the instantaneous value of secondary voltage is

$$u_2 = N_2 \frac{d\varphi}{dt} \quad \textbf{(2.2)}$$

Indices 1 and 2 indicate primary and secondary quantities, respectively. In the no-load condition, the law of induction applies and the voltage ratio (being equal to the turn ratio) will be [10]:

$$\frac{u_1}{u_2} = \frac{N_1}{N_2} \quad \textbf{(2.3)}$$

2.1 Transformer Design

Power or distribution transformers can be dry type or oil type. Depending on the cost and the environment where the transformer will be used, one of these two types is selected. An oil type transformer is mainly composed of core, windings, tank, oil and accessories. The functions of parts can be summarized respectively:

- Core and windings form the active part of a transformer. Voltage is transformed at this part.
- Tank encloses the active part and oil.
- Oil provides cooling and insulation.
- Accessories are components for protection and monitoring the transformer.

Dry type transformers have less complex structures comparing with oil type ones because they do not have oil and tank.

2.1.1 Core design

In a transformer, energy is transferred from one electrical circuit to another through the magnetic field. Transformer core made of laminated sheets provide the magnetic circuit for the flow of magnetic flux mutually linking the electrical circuits. As against the air core, iron core provides a comparatively low reluctance path to the magnetic flux with consequent benefit of (a) smaller magnetizing current, (b) increase in the total flux linkage and (c) a high ratio of mutual to leakage flux resulting in reduction of stray losses. Its design, type and manufacturing methods have significant bearing on quality, transportability, operational limitations and guaranteed technical performance of the transformer [3].

For a transformer design, the basic governing factors are:

(a) Rating of transformer and its performance,

(b) Operational conditions,

(c) Transport limitations (i.e. height, length, width, etc.)

The design of the magnetic circuit, i.e. transformer core is also based on the above considerations and it has significant bearing on the overall economy of the transformer. Based on the input voltage and frequency variations, a suitable value of flux density can be adopted to avoid any chance of core saturation under operating conditions. By increasing the operating value of magnetic flux density (magnetic loading), the net weight of core can be reduced, but this leads to corresponding increase in the core losses. One has to compute an optimum value of the magnetic flux density, keeping in view all the above considerations [3].

Design of core is initiated with calculation of limb cross-sectional area. The area depends on several factors and the expression is given as [2]:

$$q_{Fe} = C \sqrt{\frac{S}{f \cdot s \cdot B \cdot \xi} \frac{p_{Cu}}{p_{Fe}} 10^9} \quad \textbf{(2.4)}$$

where S = transformer nominal power,

f = operation frequency,

s = conductor current density,

B = magnetic flux density,

ξ = ratio between total copper and core losses,

p_{Cu} = specific copper loss,

p_{Fe} = specific core loss.

C coefficient is related with the type and geometry of the transformer and average values for this coefficient is given on table 2.1.

Table 2.1 : *C* coefficient.

	Single phase	Three phase
Cylindrical winding core type	0,45	0,40
Rectangular winding core type	0,55	0,45

Cross-sectional view of limb is determined by the power rating of the transformer. For small power ratings, rectangular cross-section is utilized. On the other hand, because of the gap between cylindrical windings and rectangular core gets more significant as power increases, stepping is applied. Up to 500 kVA transformers, simple stepping with two steps is applied while multi-step cross-section is utilized for higher power ratings [2].

Yoke cross-section area is generally 15% to 30% higher than the limb area in order to keep magnetic resistance and iron losses low on that part. Additionally, the entire core is constructed with laminated steel to avoid extreme core loss caused by eddy and Foucault losses.

After obtaining cross-sections of limbs and yokes, length of each limb and width of windows are determined. At lower and upper parts of windings, wooden supports are used for clamping, insulation and mechanical purposes. Length of a limb is the sum of winding height and height of wooden supports. For core-form transformers, the formula for width of window is given as:

$$\alpha = \frac{4}{10} \frac{w_1}{k_{Cu}} \frac{q_1}{L_s} \tag{2.5}$$

Where w_1 = number of low voltage turns,

k_{Cu} = copper fill factor of window,

q_1 = conductor area,

L_s = limb length.

Figure 2.2 [2] gives the relation between k_{Cu} and power rating of transformers.

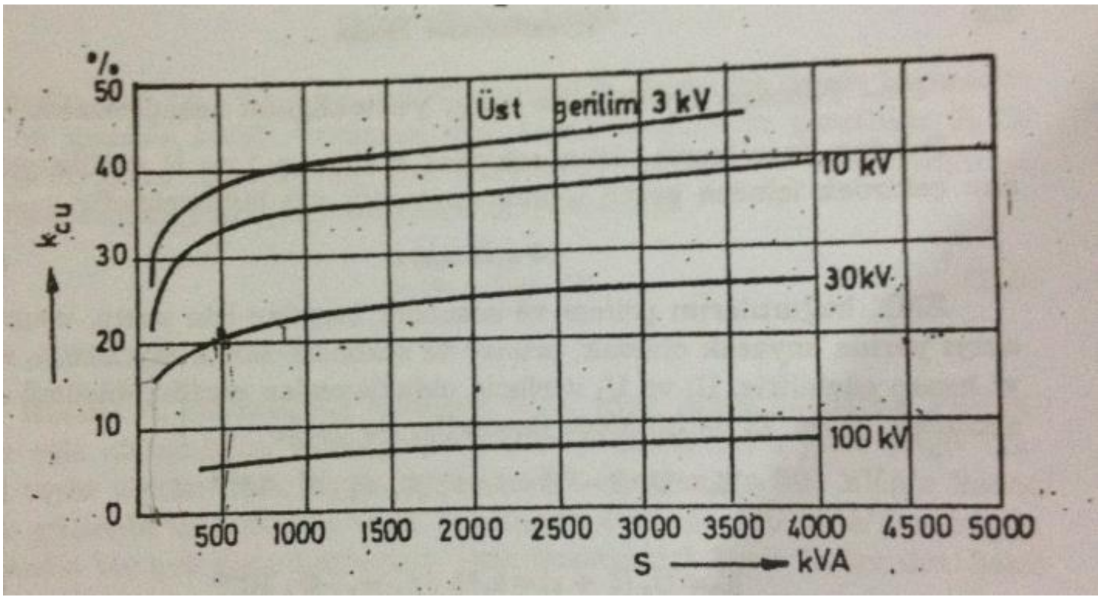

Figure 2.2 : Copper fill factor of window for core-form ONAN transformers.

The ratio between window height and width should in limitations. For core-form transformers, $2 < L_s / a < 4{,}5$ should be ensured.

2.1.2 Low voltage winding design

For core-form power transformers, there are two main methods of winding the coils. These are sketched in figure 2.3 [11]. Both types are cylindrical coils, having an overall rectangular cross-section. In a disk coil, the turns are arranged in horizontal layers called disks, which are wound, alternately out-in, in-out, etc. the winding is usually continuous so that the last inner or outer turn gradually transitions between the adjacent layers. When the disks have only one turn, the winding is a helical winding. The total number of turns will usually dictate whether the winding will be a disk or helical winding. The turns within a disk are usually touching so that a double layer of insulation separates the metallic conductors. The space between the disks is left open except for structural separators called key spacers. This allows room for cooling fluid to flow between disks, in addition to providing clearance for withstanding the voltage difference between them [11].

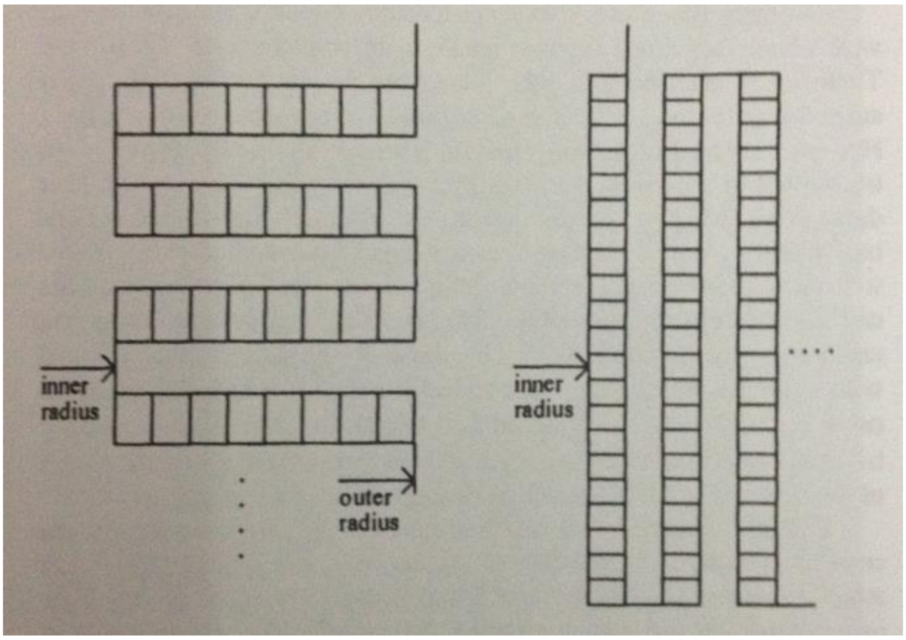

(a) (b)

Figure 2.3 : Two main methods of winding the coils: (a) disk coil, (b) layer coil.

If these coils are wound with more than one wire or cable in parallel, then it is necessary to insert cross-overs or transpositions which interchange the positions of the parallel cables at various points along the winding. This is done to cancel loop voltages induced by the stray flux. Otherwise, such voltages would drive currents around the loops formed when the parallel turns are joined at either end of the winding, creating extra losses.

For low voltage winding design, number of turns is calculated first. EMF relations for low voltage windings are:

$$E = 4{,}44 \cdot f \cdot w_1 \cdot \varphi \cdot 10^{-8} \tag{2.6}$$

$$\varphi = B \cdot q_{Fe} \tag{2.7}$$

where E = emf,

f = operation frequency,

w_1 = number of low voltage turns,

φ = total maximum magnetic flux,

B = maximum magnetic flux density,

q_{Fe} = limb cross-sectional area.

Inserting equation 2.7, into equation 2.6, w_1 is obtained.

Winding cross-sectional area is obtained by using phase current and conductor current density. Densities for copper coils are given on table 2.2. [2].

Table 2.2 : Current density for copper conductor.

Cooling type	Current density (A/mm^2)
Air (dry type)	1,7 – 2,0
ONAN	2,2 – 3,5
ONAF	3,5 – 5,0

Calculated cross-sectional area of low voltage winding is conductor area without insulation. Winding conductors have either rectangular or circular cross-section. Generally, circular conductors are used for coils with cross-sectional area under 4 mm^2 while rectangular ones are used for thicker coils. Having high phase current levels, low voltage windings of power transformers are generally constructed by rectangular conductors. Moreover, parallel branches are generally utilized for each phase of low voltage windings because of the practical difficulties of constructing coils with thin and single branch conductors. This simplifies the manufacturing process and additionally, decreases the load losses by reducing skin effect. Each parallel branch conductor of low voltage winding is covered by insulation layer and one more insulation layer is inserted radially between every two branches.

2.1.3 High voltage winding design

Same procedure is followed for high voltage winding design. Number of turns is calculated with the same formula and phase current is calculated with basic power equations. Up to a limit, conductor cross-sectional area is low enough to construct high voltage windings with circular conductors since phase current is low comparing to low voltage windings. For higher power ratings, rectangular conductors are utilized. Each conductor is covered by insulation layer and an insulation layer is inserted radially between two conductors. For protection of coils against dangerous impulsive voltages, a better insulation is utilized on the initial part of high voltage winding where the winding is connected to line.

Tapping coils are generally inserted on high voltage side in transformers in order to get more sensitive regulation results since voltage per turn is less. These coils are designed like others. Total number of turns for tapping coils is calculated with the same formula. The location where these coils will be inserted depends on the power rating of the transformer. The simplest form is obtained by dividing high voltage winding into two parts and inserting the tapping coils in the middle. It is allowed the tapping coils to be located on the upper or lower part of high voltage winding only for small power transformers [12].

2.1.4 Losses and efficiency

Transformer losses are broadly classified as no-load and load losses. No-load losses occur when the transformer is energized with its rated voltage at one set of terminals but the other sets of terminals are open circuited so that no through or load current flows. In this case, full flux is present in the core and only the necessary exciting current flows in the windings. The losses are predominately core losses due to hysteresis and eddy currents produced by the time varying flux in the core steel. Load losses occur when the output is connected to a load so that current flows through the transformer from input to output terminals. Although core losses also occur in this case, they are not part of the load losses. When measuring load losses, the output terminals are shorted to ground and only a small impedance related voltage is necessary to produce the desired full load current. In this case, the core losses are small because of the small core flux and do not significantly add to the measured losses.

Load losses are in turn broadly classified as I^2R losses due to Joule heating produced by current flow in the coils and as stray losses due to the stray flux as it encounters metal objects such as tank walls, clamps or bracing structures, and the coils themselves. Because the coil conductors are often stranded and transposed, the I^2R losses are usually determined by the d.c. resistance of the windings [11].

Temperature rise exceeds the permitted limits if losses are higher than desired values. This may result with damage in winding insulation and outage of transformer because of internal short circuit. In order to avoid this, after designing core and windings, no-load and load losses are calculated before manufacturing to keep sure they are in accordance with desired technical characteristics. The design is revised if losses are over desired level.

For low voltage winding,

$$r_2 = \frac{\mathrm{l}_{\mathrm{m2}} \cdot w_2 \cdot p}{\mathrm{q}_2} \tag{2.8}$$

where r_2 = low voltage winding resistance,

l_{m2} = average length per turn,

w_2 = number of low voltage turns,

p = specific resistivity of winding conductor,

q_2 = conductor cross-sectional area.

Coefficient for increase in resistance of low voltage side for rectangular conductor is,

$$K_{\mathrm{r}} = 1 + \frac{\mathrm{m}^2 - 0{,}2}{9} \quad \xi^4 \tag{2.9}$$

$$\xi = 2 \cdot \pi \cdot \mathrm{h} \sqrt{\frac{\mathrm{n} \cdot \mathrm{b} \cdot \mathrm{f}}{\mathrm{l}_{\mathrm{s}} \cdot p \cdot 10^5}} \tag{2.10}$$

where h = radial width of each conductor,

n = number of axially assembled conductors,

m = number of axially assembled conductors,

b = axial height of each conductor,

f = operation frequency,

l_s = L + 2H using the dimensions given on figure 2.4 [2].

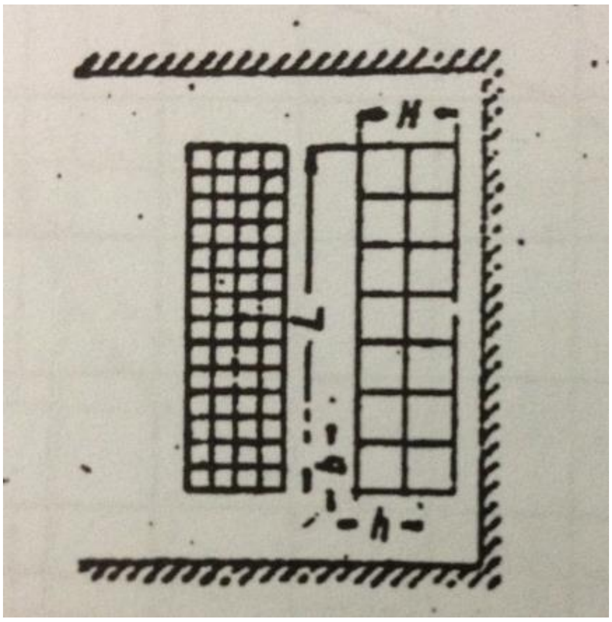

Figure 2.4 : Winding dimensions.

Loss in low voltage windings is calculated as:

$$P_{cu2} = 3 \cdot I_2^{\ 2} \cdot (r_2 \cdot K_r) \qquad \textbf{(2.11)}$$

Extra losses caused by the solder and connection points are taken into account by a coefficient depending on the current. Table (no ver) gives the coefficient for these extra losses.

Table 2.3 : Extra losses.

I (A)	100	200	300	500	700	1000	1500
% Extra losses	7,5	10	12	15	17.5	20	25

P_{cu2} is multiplied by (100+%Extra loss)/100 for obtaining low voltage winding copper loss.

For high voltage winding,

$$r_1 = \frac{l_{m1} \cdot w_1 \cdot p}{q_1} \qquad \textbf{(2.12)}$$

where r_1 = high voltage winding resistance,

l_{m1} = average length per turn,

w_1 = number of high voltage turns,

p = resistivity of winding conductor,

q_1 = conductor cross-sectional area.

Loss in high voltage windings is calculated similarly:

$$P_{cu2} = 3 \cdot I_2^{\ 2} \cdot (r_2 \cdot K_r) \tag{2.13}$$

and total copper loss is

$$P_{cu} = P_{cu1} + P_{cu2} \tag{2.14}$$

Total core loss is the sum of loss in limbs and yokes. Limbs and yokes are in different weights and they operate at different maximum flux densities. Loss of each region is calculated separately and total loss is obtained by summation. Loss per weight in steel laminations is:

$$p_{fe} = \zeta \cdot p_{10} \cdot \left(\frac{B}{10000} \right)^2 \tag{2.15}$$

where ζ = core loss factor (caused by constructional issues),

p_{10} = steel loss factor,

B = maximum flux density.

After obtaining p_{fe} in watt/kg for limbs and yokes, total loss is obtained by multiplying these values by related masses in kg.

$$P_{fe} = m \cdot p_{fe} \tag{2.16}$$

Transformer instantaneous efficiency is the ratio between output power and input power.

$$\eta = \frac{P_{out}}{P_{in}} = \frac{P_{out}}{P_{out} + P_{cu} + P_{fe}} \quad \textbf{(2.17)}$$

where P_{out} = output power,

p_{10} = steel loss factor,

P_{cu} = copper loss,

P_{fe} = core loss.

Unlike rotating machines, transformers do not have mechanical losses caused by friction. Thanks to this, transformer efficiency is much higher than that of rotating machines.

2.1.5 Mechanical supports and clamping equipment

Insulation between windings and core is provided by insulation paper on conductors, wooden separation rods between high voltage and low voltage windings and wooden supports inserted between upper and lower end of windings and core. Radial height of wooden rods is a function of high voltage. Similarly, height of upper and lower supports depends on the high voltage of transformer. Besides the function of wooden parts providing insulation between different voltage levels, they are utilized in order to support windings mechanically. Upper and lower supports between windings and core provide support against axial forces. Additionally, since the transformer core is constructed by using thin layers of steel, clamping is applied on core in order to hold the layers together. Upper and lower clamps on core also protect the windings with wooden supports.

2.2 Forces in Transformers

The typical flux pattern in a two winding transformer of core-type is given in figure 2.5 [3]. The flux lines are almost axial at the middle of the winding and start bending in the radial direction as we move towards the winding ends. In other words, the axial component is predominant along the height of the winding, except at the winding ends (top and bottom), where the radial component becomes significant. The direction of current in the winding conductors is perpendicular to the flux lines, thus resulting in the axial and radial component of forces.

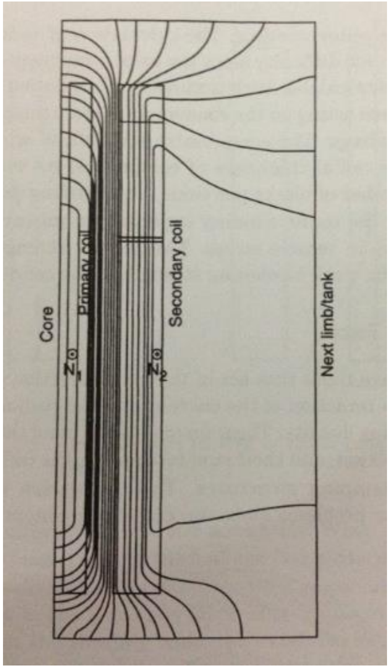

Figure 2.5 : The typical flux pattern in a two winding transformer.

Forces are produced due to the interaction of the current and the magnetic flux density vectors. Thus, in general, the force vector can have any direction. Nevertheless, it is easier to speak of the radial forces and axial forces in a transformer, since these two components of the force can be calculated and analyzed independently. Also, the two components have influence on different parts of the total and it is necessary to obtain two components for design purposes [3].

Current carrying conductors passing through a magnetic field are subjected to electromagnetic forces. These forces can be calculated using equation **2.18**.

$$\vec{f} = \vec{J} \; x \; \overrightarrow{B} \qquad \textbf{(2.18)}$$

where $\vec{f}$ = force density vector,

$\vec{J}$ = current density vector,

$\vec{B}$ = leakage flux density vector.

In transformers, since current carrying low and high voltage windings are in leakage flux and there is 180° phase shift between currents passing through low and high voltage windings (neglecting no load current), windings push each other radially because of axial component of leakage flux [6]. By these radial forces, oil gap between low and high voltage windings tries to get wider. High voltage winding copper length gets longer while that of low voltage winding get shorter. In conclusion, insulation around conductors is damaged and several electrical faults are observed.

In transformers with low and high voltage windings in same length, axial forces caused by radial component of leakage flux are very small. They are almost zero under normal operation conditions. These forces can have extreme values under short circuit if winding lengths are different. To avoid this, required measures should be taken during project and construction phases [6]. In this study, it is assumed that winding lengths are equal and effect of axial forces is negligible. Additionally, effect of axial forces is suppressed by clamping equipment.

2.3 Short Circuit

2.3.1 Short circuit types

In figure 2.6 [4], most frequent short circuit types for three-phase power system are given.

The short circuit faults are called shunt faults; open circuits, which may be caused by broken conductors, for instance, are categorized as series faults [5]. In this study, effects of short circuits (shunt faults) on transformers are analyzed. This type of faults can be imagined as a load with small impedance (or zero impedance) connected in parallel to the system loads. The operation of a power system departs from normal after the occurrence of a fault. Faults give rise to abnormal operating conditions – usually excessive currents and voltages at certain points on the system – , which are guarded against various types of protective equipment [5].

Most of the faults that occur on power systems are unsymmetrical faults, which may consist of unsymmetrical short circuits, unsymmetrical faults through impedances or open conductors. Unsymmetrical faults occur as single line-to-ground faults, line-to-line faults, or double line-to-ground faults. The path of the fault current from line to

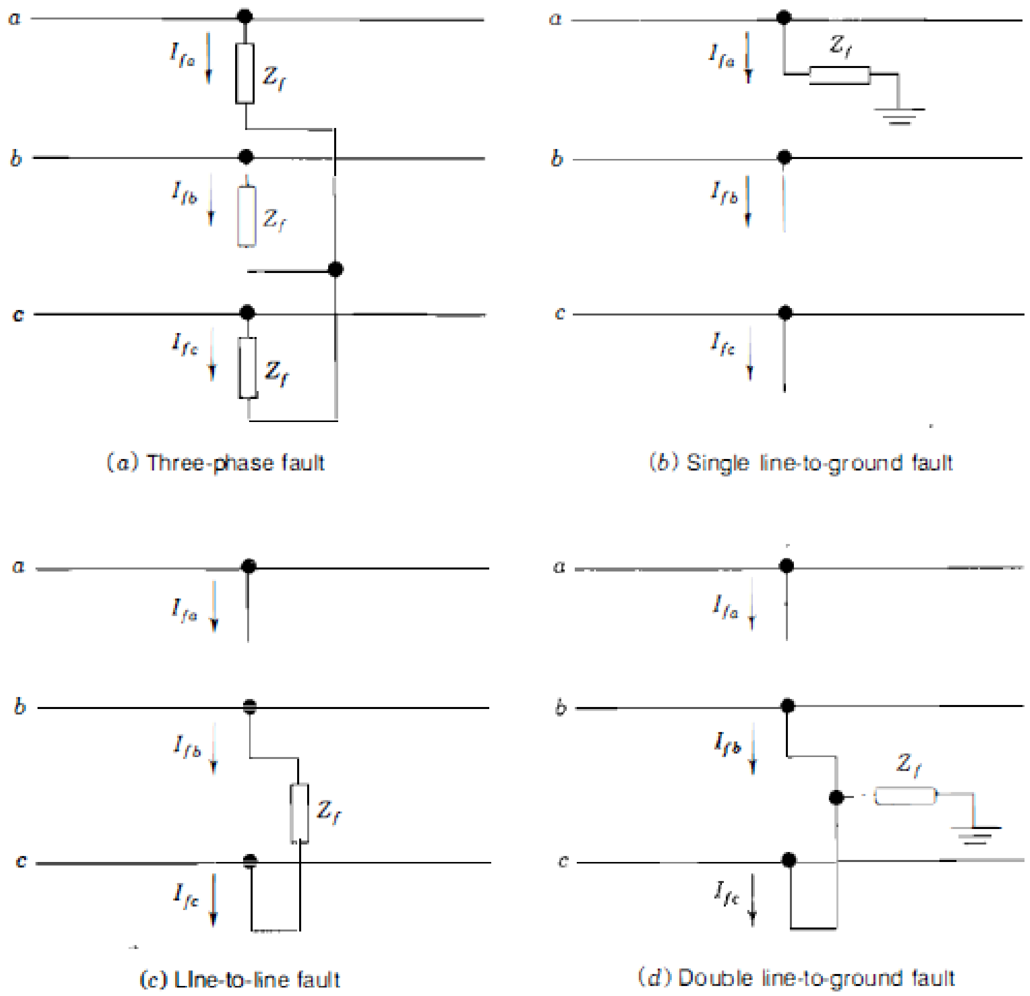

Figure 2.6 : Faults in three phase power system.

line or line to ground may or may not contain impedance. One or two open conductors result in unsymmetrical faults, through either the breaking of one or two conductors or the action of fuses and other devices that may not open the three phases simultaneously. Since any unsymmetrical fault causes unbalanced currents to flow in the system, the method of symmetrical components is very useful in an analysis to determine the currents and voltages in all parts of the system after the occurrence of the fault [4].

The symmetrical short-circuit current for a three phase two winding transformer is given by

$$I = \frac{U}{(Z_t + Z_s)\sqrt{3}} \qquad \textbf{(2.19)}$$

where U = rated voltage,

Z_t = short circuit impedance of the transformer,

Z_s = short circuit impedance of the system.

In the case of transformers of up to 3150 kVA, Z_s can be neglected if it is lower than $0.05\,Z_t$. In IEC Publication 76-5 the typical impedance voltages of transformers are given as listed in table 2.4. from the percentage impedance voltage u_k, rated voltage U and rated power S of the transformer, its short circuit impedance in ohms is given as

$$Z_t = \frac{u_k \cdot U^2}{100\ S} \qquad \textbf{(2.20)}$$

Depending on the connection of transformer windings, the symmetrical short-circuit currents of line-to-line, line-to-earth and double-earth faults of the transformer are not equal in every case to the value obtained from formula **2.19** the short circuit currents assume the following values in the various cases most often occurring in practice:

(a) In a transformer of star/zig-zag or delta/zig-zag connection, a line-to-earth fault between neutral point and a phase terminal of the zig-zag winding causes the short-circuit current to increase with respect to the symmetrical value by a factor of about 1,5.

(b) In a transformer of star/star connection with neutrals brought out on both sides having a delta connected tertiary or a stabilizing winding, a line-to-earth fault in the secondary circuit will cause a short-circuit current which is of magnitude

$$I = \frac{U}{\frac{2}{3} Z_s + Z_d} \qquad \textbf{(2.21)}$$

where U = rated voltage,

Z_s = short-circuit impedance between the two star connected windings,

Z_d = short-circuit impedance between short-circuited winding and the delta-connected tertiary or stabilizing winding.

The line-to-earth fault current is lower than the three phase fault if $Z_d > Z_s / \ 3$.

Table 2.4 : Impedance voltages of two-winding transformers.

Rated power (kVA)	
up to 630	4
631 to 1250	5
1251 to 3150	6,25
3151 to 6300	7,15
6301 to 12500	8,35
12501 to 25000	10
25001 to 200000	12,5
200001 and above	subject to agreement

Generally, this latter condition is not satisfied when the transformer is fed from its winding of largest diameter, the fault occurs in its centrally arranged winding, and its tertiary (or stabilizing) winding is of the smallest diameter. Generally, too, power systems are designed to keep short circuit levels within reasonable limits; therefore, if fault currents are to be restricted, reactors are inserted in the delta-connected circuits of transformers in order to increase their impedance voltage.

(c) the magnitude of short-circuit currents associated with line-to-line faults on the delta side of star/delta and delta/delta connected transformers is the same as that occurring in the case of a symmetrical fault. In a delta/star transformer (with neutral brought out) and in star/star transformers with neutrals brought out on both sides, the magnitude of single line-to-earth fault currents is closely equal to that of a three-phase fault.

(d) In a star/star connected transformer the short-circuit current of a line-to-line fault is $\sqrt{3}/2 = 0{,}866$ times the value of the symmetrical fault current. With a fault between two phases on the star-connected side of a delta/star transformer, the secondary- side fault current is $\sqrt{3}/2 = 0{,}866$ times the symmetrical short-circuit current. Finally, in star/star connection with no neutral brought out on the input side, the fault current associated with a short circuit between one phase on the secondary side and the neutral terminal is

$$I = \frac{U}{\frac{2}{3}Z_t + Z_0} \tag{2.22}$$

where Z_t = short-circuit impedance pertaining to the symmetrical three-phase fault,

Z_0 = zero-sequence impedance of the transformer.

The zero-sequence impedance, with no delta winding being present, is much higher than the positive-sequence impedance (the impedance pertaining to the symmetrical three-phase fault is the positive-sequence impedance), therefore the short circuit current calculated from the former formula is below what would arise in the symmetrical case [10].

2.3.2 Time dependent short circuit current

The transformer and the remaining power system have resistive and reactive character, which gives the system dynamic behavior. In order to approach the problem of calculating the initial current when a system is short-circuited, consider what happens when an ac voltage is applied to a circuit containing constant values of resistance and inductance. Let the applied voltage be $V_{\max}\sin(wt+\alpha)$, where t is zero at the time of applying the voltage. Then, α determines the magnitude of the voltage when the circuit is closed. If the instantaneous voltage is zero and increasing in a positive direction when it is applied by closing a switch, α is zero. If the voltage is at its positive maximum instantaneous value, α is $\pi/2$. The differential equation is

$$V_{\max}\sin(wt+\alpha) = R\cdot i + L\cdot\frac{di}{dt} \tag{2.23}$$

The solution of this equation is

$$i = \frac{V_{max}}{|Z|} \sin(wt + \alpha - \theta) + e^{-\frac{Rt}{L}} \sin(\alpha - \theta) \quad \textbf{(2.24)}$$

where

$$|Z| = \sqrt{R^2 + (wL)^2} \quad \textbf{(2.25)}$$

$$\theta = \tan^{-1}(wL/R) \quad \textbf{(2.26)}$$

The first term of Eq. **2.24** varies sinusoidally with time. The second term is nonperiodic and decays exponentially with a time constant L/R. This nonperiodic term is called the dc component of the current. We recognize the sinusoidal term as the steady-state value of the current in an RL circuit for the given applied voltage. If the value of the steady-state term is not zero when $t = 0$, the dc component appears in the solution in order to satisfy the physical condition of zero current at the instant of closing the switch . Note that the dc term does not exist if the circuit is closed at a point on the voltage wave such that $\alpha - \theta = 0$ or $\alpha - \theta = \pi$. Figure 2.7(a) [4] shows the variation of current with time according to Eq. **2.24** when $\alpha - \theta = 0$. If the switch is closed at a point on the voltage wave such that $\alpha - \theta = \pm\pi/2$, the dc component has its maximum initial value, which is equal to the maximum value of the sinusoidal component. Figure 2.7(b) [4] shows current versus time when $\alpha - \theta = -\pi/2$. The dc component may have any value from 0 to $V_{max}/|Z|$, depending on the instantaneous value of the voltage when the circuit is closed and on the power factor of the circuit. At the instant of applying the voltage the dc and steady-state components always have the same magnitude but are opposite in sign in order to express the zero value of current then existing [4].

2.3.3 Short circuit forces

Magnitude of radial forces acting on low and high voltage windings is calculated by using axial component of leakage flux in oil gap, which is

$$B = \mu_0 \frac{w \cdot I_k}{h} K \quad \textbf{(2.27)}$$

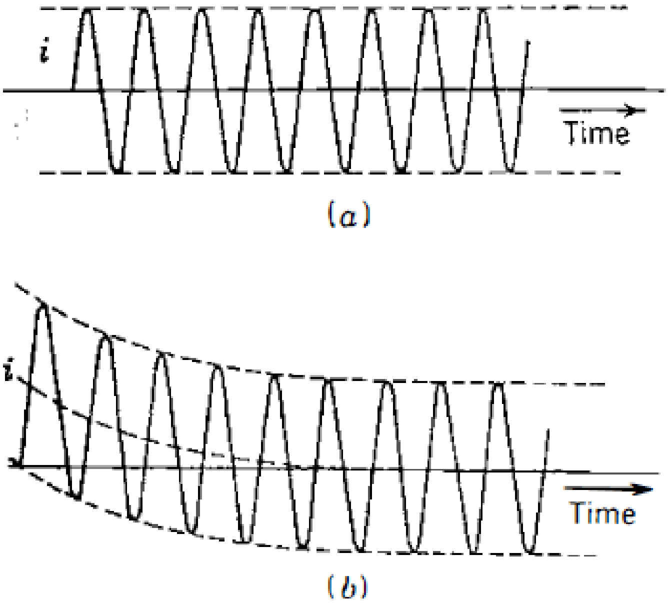

Figure 2.7 : Current as a function of time in an RL circuit for: (a) $\alpha-\theta=0$;

(b) $\alpha-\theta=-\pi/2$

where I_k = short circuit instantaneous current,

w = number of winding turns,

h = low and high voltage winding heights (in meters),

K = Rogowski correction factor [6].

Correction factor is calculated as:

$$K = 1 - \frac{s}{\pi h}\left(1 - e^{-\frac{\pi h}{s}}\right) \qquad \textbf{(2.28)}$$

μ_0 is permeability of air and its value is $1{,}256 \;\; x \;\; 10^{-6} \;\; \left[\frac{H}{m}\right]$

Since each winding is covered by half of peak flux given on figure 2.8,

$$F_n = I_k w \frac{B_m}{2} U_m \quad [N] \qquad \textbf{(2.29)}$$

where U_m is avarage winding length.

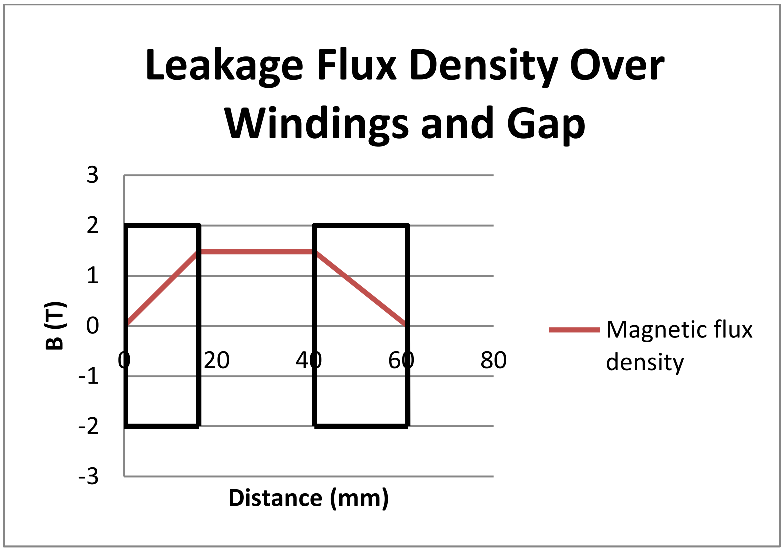

Figure 2.8 : Leakage flux density

Inserting equation **2.27** into equation **2.29**,

$$F_n = \mu_0 \frac{I_k{}^2 w^2}{2h} U_m K \qquad [N] \tag{2.30}$$

The typical waveforms of the short circuit current and force are shown in figure 2.9 [1]. Thus, with a fully offset current the fundamental frequency component of the force is dominant during the initial cycles as seen from the figure [1].

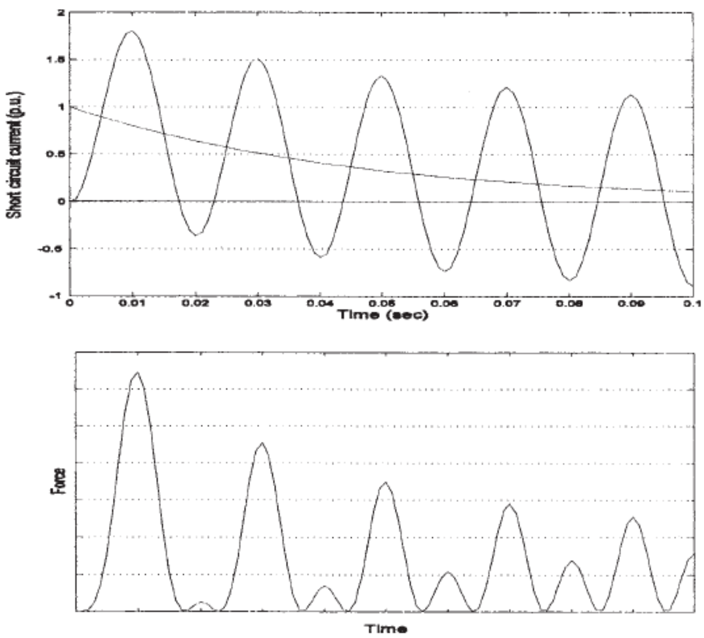

Figure 2.9 : Typical waveforms of short circuit current and force

3. TRANSFORMER DESIGN IN DIFFERENT GEOMETRIES

3.1 Design Criteria

Since the effect of winding geometry on forces and deformation of active part caused by these forces is analyzed in this study, only the active part is designed. Research conducted before shows that the effect of remaining parts on analyzed points is negligible [13]. Additionally, it is assumed that designed transformers withstand stresses except the analyzed ones.

Distribution transformers with Dyn vector group are widely used in power networks. Design, analysis and simulations will be done for this type of transformers in this study. An oil immersed ONAN (oil natural air natural) Dyn5 distribution transformer with technical characteristics given on Table 3.1 is designed in three different geometries.

Table 3.1 : ONAN transformer technical characteristics.

Quantity	Value	Unit
Power	250,00	kVA
High Voltage	34,50	kV
Low Voltage	0,40	kV
Impedance	4,00	%
Frequency	50,00	Hz
Load Power Factor	0,85	-
Copper Loss	4.375,00	W
Core Loss	1.625,00	W

First design is done by usage of cylindrical windings since this geometry is commonly used for practical transformers operating in power system. Then, the elliptical one is designed with a specified ellipse ratio. Finally, a square winding transformer is designed.

Design procedure and formulas given in Elektrik Makinaları Dersleri textbook [2] is used for design. Effect of regulating coils is not covered in this study and the transformers are designed without tap windings. Additionally, design constraints used for transformer with given specifications are obtained from the subject book and are given on table 3.2. In order to observe the effect of design geometry better, windings are designed to arrange height/width ratio close for three types of designs.

Table 3.2 : Design constraints.

Quantity	Value	Unit
Copper current density	2,60	A/mm2
Copper loss	18,25	W/kg
Core loss factor	1,15	-
Magnetic flux density	13.900,00	Gauss
Core loss	1,30	W/kg
Geometry constant (cylindrical)	0,40	-
Geometry constant (elliptical)	0,42	-
Geometry constant (square)	0,44	-

3.2 Design with Cylindrical Windings

First design is made by cylindrical windings. To achieve this, core, low voltage and high voltage windings are designed respectively and the design verification is done at the end. Since the thermal analysis is out of the scope of this study, tank and radiator design are not done.

Cross-sectional area of core is 228 cm^2. In order to fill the low voltage winding cylinder, stepping is applied. For this design, two-pitch stepping is applied and the top view of core limb is obtained as given on figure 3.1(a). On the other hand, cross-sectional area of yoke is 20 % more than the one of limb because the magnetic flux density is 20 % less. Sınce the core depth is same for limb and yoke, height is 20 % more for yoke. Top view of yoke is given on figure 3.1(b)

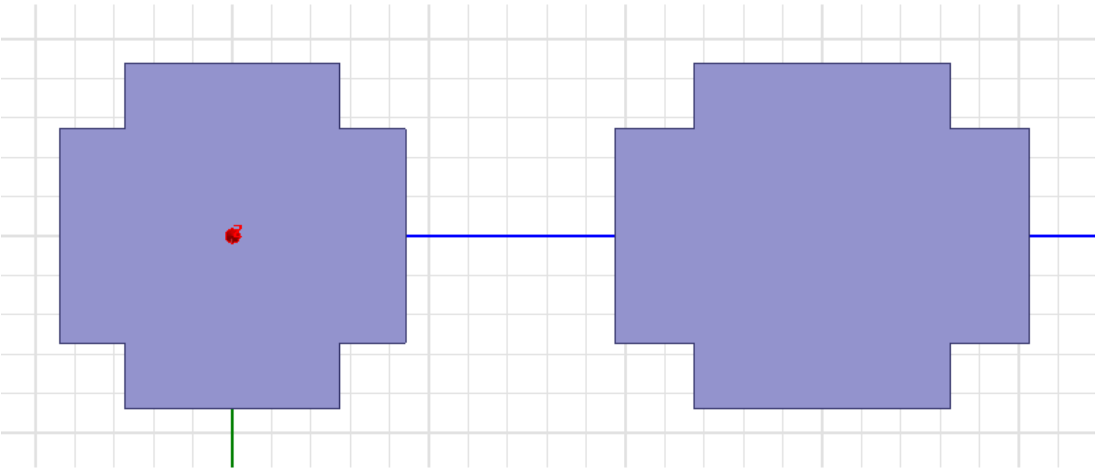

(a) (b)

Figure 3.1 : Cross section of : (a) limb, (b) yoke for cylindrical design.

Core is made of steel with laminations in order to minimize no load loss (core loss). Lamination factor is 0,95 and steel thickness is 0,5 mm.

After designing core, windings are designed. Before low voltage windings, 4 mm insulation is wound on core. Then 33 turns/limb low voltage winding is used. Low voltage current is 360,8 A which is high for a single branch. Assuming current carrying capability of a single branch to be 125 A, three single rectangular branches are used for low voltage winding. Between low voltage and high voltage windings, separation rods with 25 mm thickness are used for insulation. High voltage winding is 4904 turns/limb and circular conductors are used. Using related thickness values given in textbook, windings are designed and given on figure 3.2 with core. On figure, 4 mm insulation paper, LV winding, separation rods and HV windings are seen on core respectively.

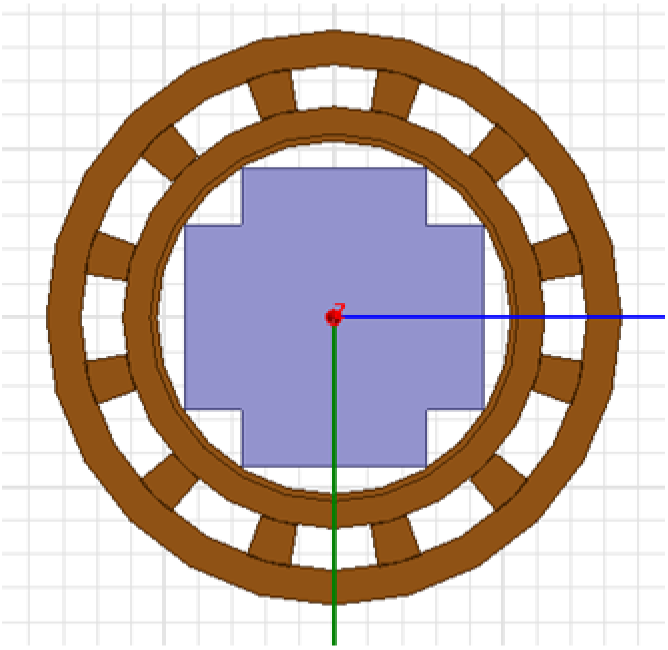

Figure 3.2 : Cross-section of limb with core, insulation and windings for cylindrical design.

Design verification is needed at the end of cylindrical design to ensure the designed transformer meets the required specifications. On Table 3.3, results for designed transformer are given. They are acceptable according to book [2].

Table 3.3 : Design verification for cylindrical design.

Quantity	Value	Unit	Required
Window height/window width	2,94	A/cm	2 < x < 4,5
Total copper loss	3.861,55	W	4.375,00
Total core loss	1.722,73	W	1.625,00
Temperature difference between lv and oil	18,41	°C	x < 20
Temperature difference between hv and oil	17,24	°C	x < 20
Impedance	4,10	%	4

3.3 Design with Elliptical Windings

Second design is made by elliptical windings. The method and the formulas used at cylindrical type design is also used for this type by being adapted at necessary points. To perform elliptical winding transformer design, an "ellipse equation" is specified first. Given in equation **3.1**, *a* and *b* determine the character of ellipse.

"a/b" coefficient and radius defines the ellipse and different designs can be obtained by arranging this coefficient.

$$\frac{x^2}{a^2}+\frac{y^2}{b^2}=r^2 \tag{3.1}$$

This coefficient is selected to be "1,4" for this study. The remaining part of design is done according to this value. Using the cross-sectional area of core, which is 239 cm^2, top view of limb is obtained as given on figure 3.3(a). Core material properties are same as cylindrical design. Yoke cross-section is given on figure 3.3(b).

Low voltage winding is 31 turns/limb. The difference between turns/limb with cylindrical design is the result of different geometry constants. Separation rods with 25 mm thickness are used again. High voltage winding is 4678 turns/limb and circular conductors are used. Using related thickness values given in textbook, windings are designed and given on figure 3.4.

On Table 3.4, results for designed transformer are given. They are acceptable according to book [2].

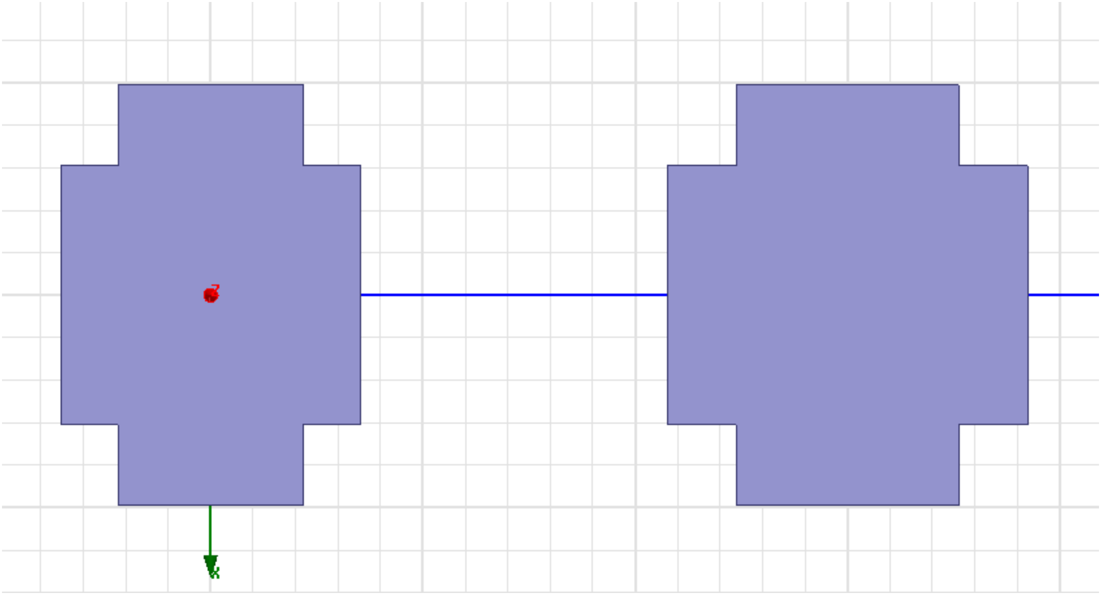

(a) (b)

Figure 3.3 : Cross section of : (a) limb, (b) yoke for elliptical design.

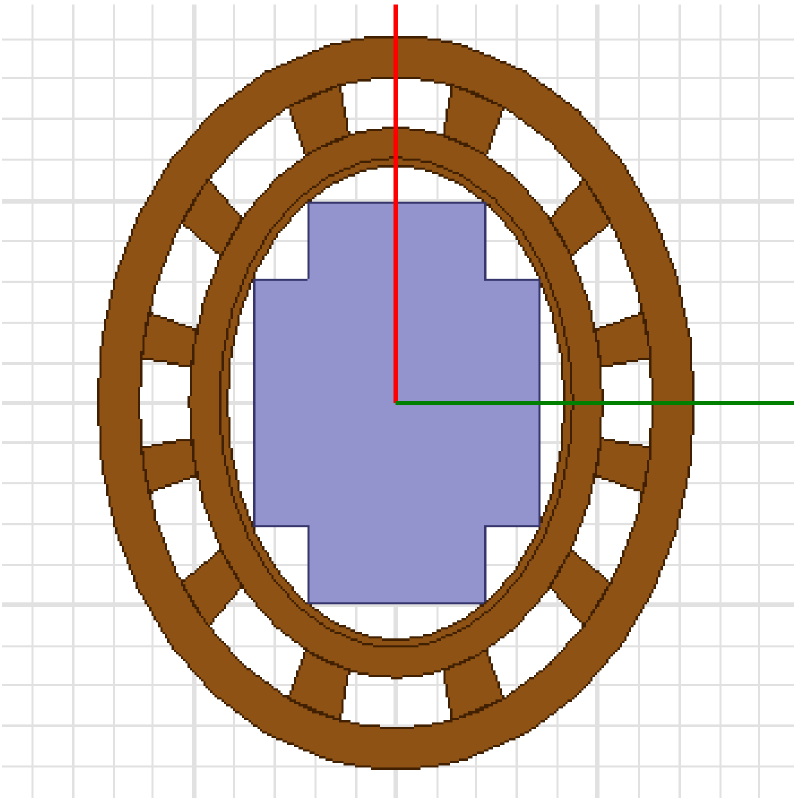

Figure 3.4 : Cross-section of limb with core, insulation and windings for elliptical design.

Table 3.4 : Design verification for elliptical design.

Quantity	Value	Unit	Required
Window height/window width	2,93	A/cm	2 < x < 4.5
Total copper loss	3.547,11	W	4.375,00
Total core loss	1.674,57	W	1.625,00
Temperature difference between lv and oil	18,04	°C	x < 20
Temperature difference between hv and oil	16,44	°C	x < 20
Impedance	3,89	%	4

3.4 Design with Square Windings

Square design is a special type for rectangular winding transformers. For this design, stepping is not needed. For cylindrical and elliptical winding transformer design, core was stepped since the windings were not straight and a gap is formed between windings and core. Windings are straight and can be filled with core without stepping for rectangular case. Core cross-sectional area is calculated like cylindrical one. It is 251 cm^2 and side length of square is 15,8 cm. Core material properties are same as cylindrical design. Limb and yoke cross sections are given on figures 3.5(a) and 3.5(b) respectively.

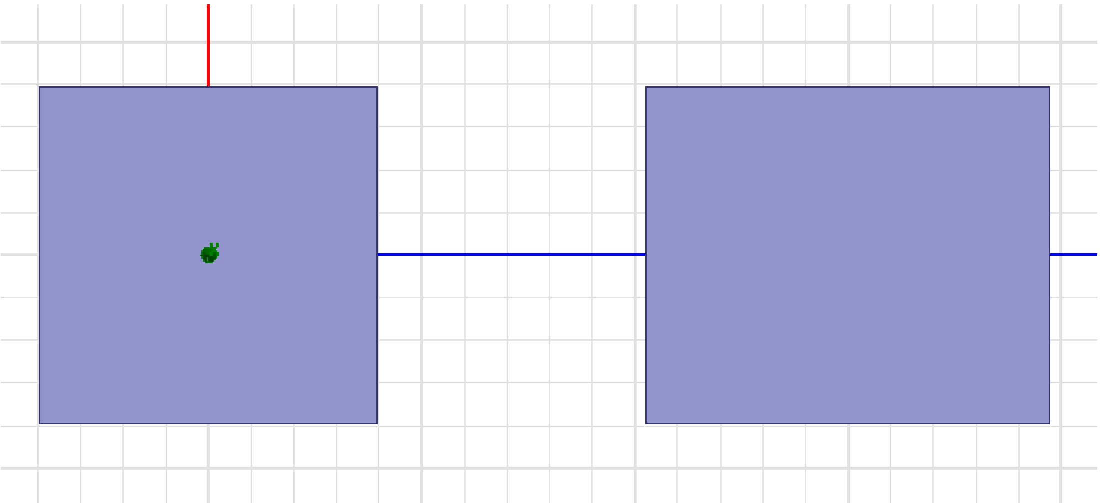

(a) (b)

Figure 3.5 : Cross section of : (a) limb, (b) yoke for square design.

Low voltage winding is 30 turns/limb. High voltage winding is 4454 turns/limb and circular conductors are used. Low voltage conductors are rounded on corners with 15 mm inner radius. Using related thickness values given in textbook, windings are designed and given on figure 3.6.

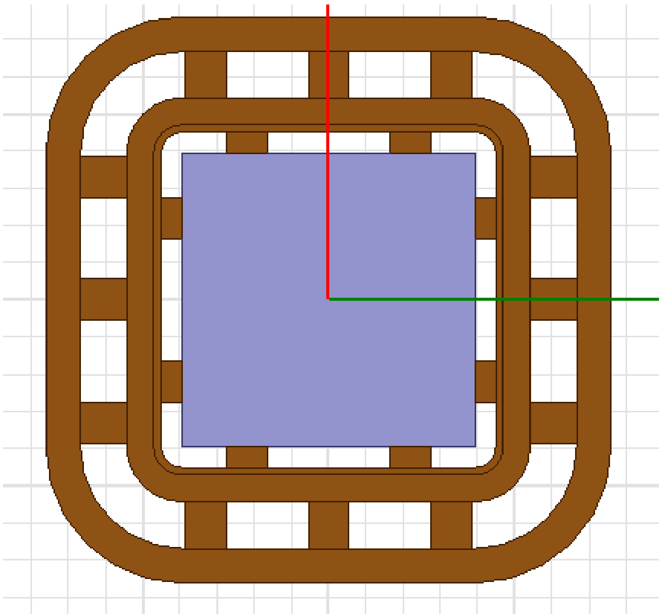

Figure 3.6 : Cross-section of limb with core, insulation and windings for square design.

On Table 3.5, results for designed transformer are given. They are acceptable according to book [2].

Table 3.5 : Design verification for square design.

Quantity	Value	Unit	Required
Window height/window width	2,93	A/cm	2 < x < 4,5
Total copper loss	3.970,46	W	4.375,00
Total core loss	1.799,87	W	1.625,00
Temperature difference between lv and oil	17,08	°C	x < 20
Temperature difference between hv and oil	16,07	°C	x < 20
Impedance	4,04	%	4

As seen on equation **2.30**, radial force depends on the mean radius and height of windings assuming other variables are fixed. To observe effect of winding geometry on force and deformation on structure, design of transformers is done keeping the ratio between total radial thickness of windings and height close in this study. Table 3.6 gives total thicknesses, heights and ratio for three designs.

Table 3.6 : Total winding thicknesses, heights and ratio.

	Total radial thickness (mm)	Height (mm)	Ratio
Cylindrical	61,39	505,56	0,121
Elliptical	60,16	486,70	0,124
Square	58,06	493,80	0,118

4. ELECTROMAGNETIC ANALYSIS

After three types of transformers with different winding geometries are designed, forces acting on windings under short circuit condition will be obtained.

4.1 Analytical Force Calculation

Using the formula given in part 2, radial force for designed cylindrical winding transformer is calculated. Short circuit currents are same for thee designs. Worst-case analysis is done by using maximum current in calculations and simulations. Additionally, equivalent impedance of remaining system will be assumed zero. Maximum short circuit peak current is observed when $\alpha - \theta = \pi/2$ in equation **2.24**. On high voltage side,

$$i = \frac{V_{\max}}{|Z|}\sin(wt + \alpha - \theta) + e^{-\frac{Rt}{L}}\sin(\alpha - \theta) = 170{,}77 \text{ A}$$

at t=0 s. This is the value to be used in worst-case analysis although, in practice, the entire system parameters will provide the short circuit current to be less. The initial and maximum instant force on windings will be calculated using this value.

Using this current in equation **2.30** and ignoring the effect of correction factor K since it is around 1,

$$F_n = \mu_0 \frac{I_k^{\,2} w^2}{2h} U_m K \quad \approx \mu_0 \frac{I_k^{\,2} w^2}{2h} U_m = 1{,}256 \ x \ 10^{-6} \ \frac{170{,}77^2 \cdot 4904^2}{2 \cdot (0{,}505)} (\pi \cdot 0{,}317)$$

$$F_n = 868.563{,}31 \quad [N]$$

This force is the maximum total radial force on high voltage winding of cylindrical design transformer.

4.2 Calculation by Finite Element Method

The formula for calculation of forces on cylindrical windings is obtained straightforward and forces are assumed to be uniformly distributed around the cylinder. On the contrary, it is hard to formulize forces on elliptical and square windings. Calculation of forces for elliptical and square design is more complicated since the structures of windings are not uniform around core. Additionally, force densities are not uniform for these geometries because of relatively sharp surfaces. In order to obtain force distribution on transformer windings for three types of designs, ANSYS Maxwell, a FEM (finite element method) based software is utilized.

In reference (13), worst-case analysis is performed by using the instant when center phase high voltage and low voltage currents are maximum. At this time instant, half of the center phase current with 180° phase shift passes through outer phase windings. Applying the same procedure, short circuit currents of HV and LV windings for three designs are given on table 4.1.

Table 4.1 : Short circuit currents when center phase currents are maximum.

Total current (A)			
Center phase		Outer phases	
LV	HV	LV	HV
-25.515,24	170,77	12.757,62	-85,38

4.2.1 Calculation for cylindrical windings

Three-dimensional drawing of the entire active part of transformer is obtained first in order to perform simulation. This drawing given on figure 4.1 includes core, windings, lower and upper supports, clamping equipment and insulation rods between high voltage and low voltage windings.

Since the relative permeability of oil and wood is around 1,00 and the parts made of these materials have no effect on magnetic analysis, the entire structure is simplified and only core and windings are used in simulation. The simplified version of structure is given on figure 4.2.

Running the simulation, magnetic flux density on the region where windings are located is obtained and given on figure 4.3.

As expected, magnetic flux density on center limb is highest in three limbs. Additionally, inner shell of low voltage windings and outer shell of high voltage windings are under zero magnetic flux. Maximum flux density is on air gap between outer shell of low voltage winding and inner shell of high voltage winding of same limb for three limbs. Figure 4.4 shows the magnetic flux density on low voltage windings of three limbs. It is almost uniform along the z-axis on each limb. A small decrease is recorded on top and bottom ends.

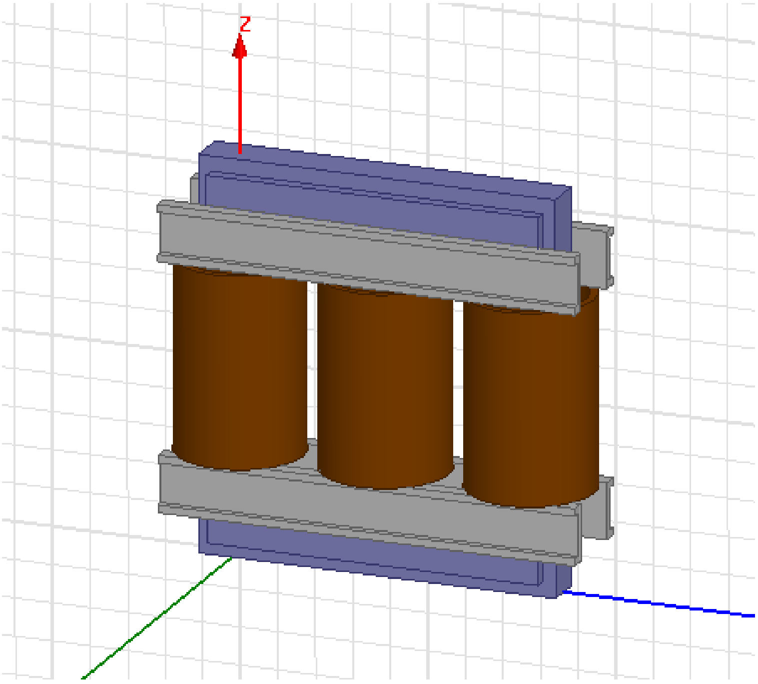

Figure 4.1 : Entire active part of cylindrical design.

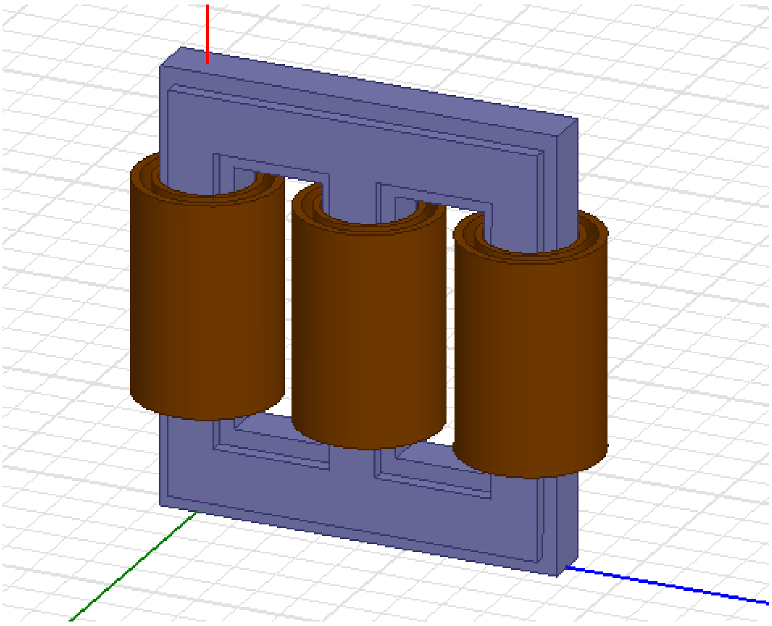

Figure 4.2 : Simplified version of cylindrical design.

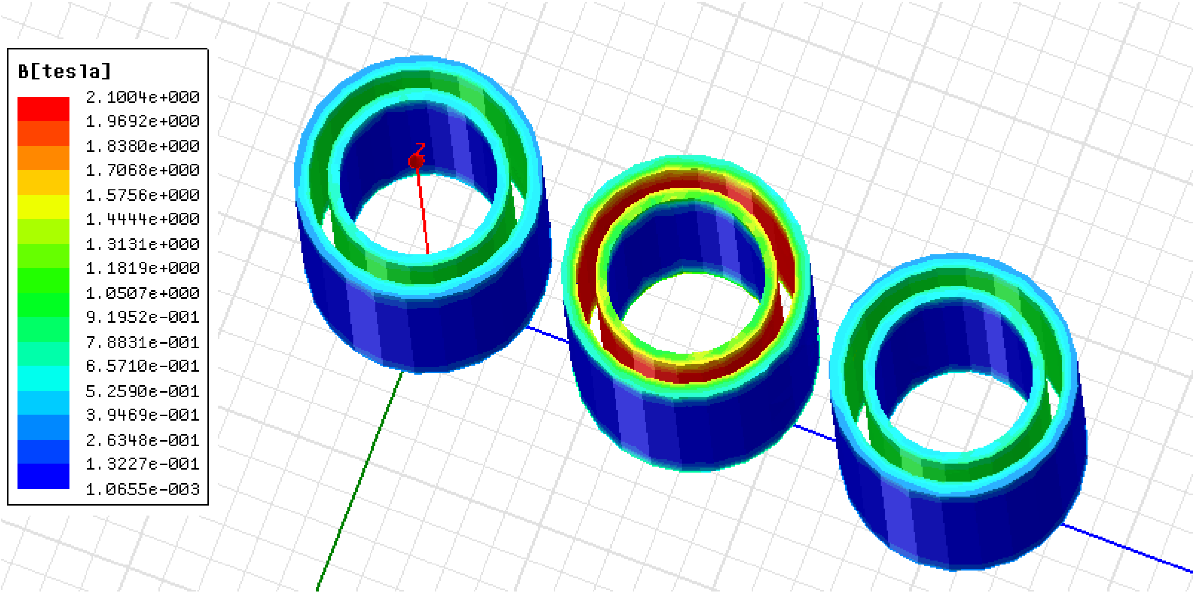

Figure 4.3 : Magnetic flux density around cylindrical design windings.

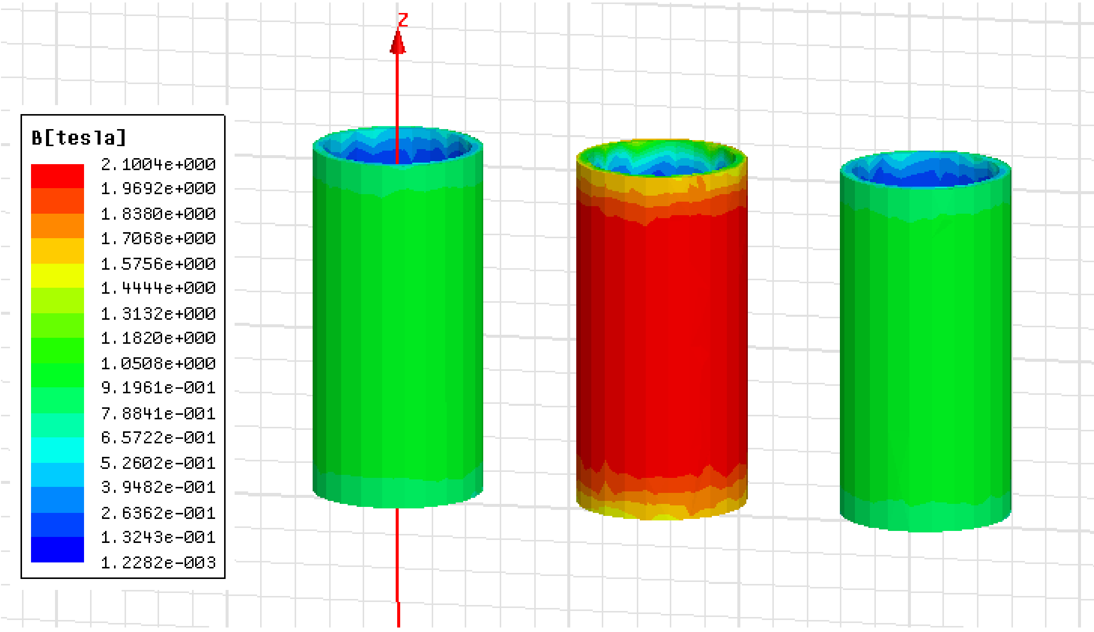

Figure 4.4 : Magnetic flux density on cylindrical design LV windings.

Similarly, magnetic field intensity distribution is given on figure 4.5. It has similar characteristics with magnetic flux density noting that the vector directions for B and H are not same.

After obtaining B and H, forces on windings will be obtained. Output of the Maxwell software to be used for this aim is volume force density in N/m^3. Multiplying these volume force density values by winding thicknesses, winding height and average winding circumference, total force on windings are obtained in N.

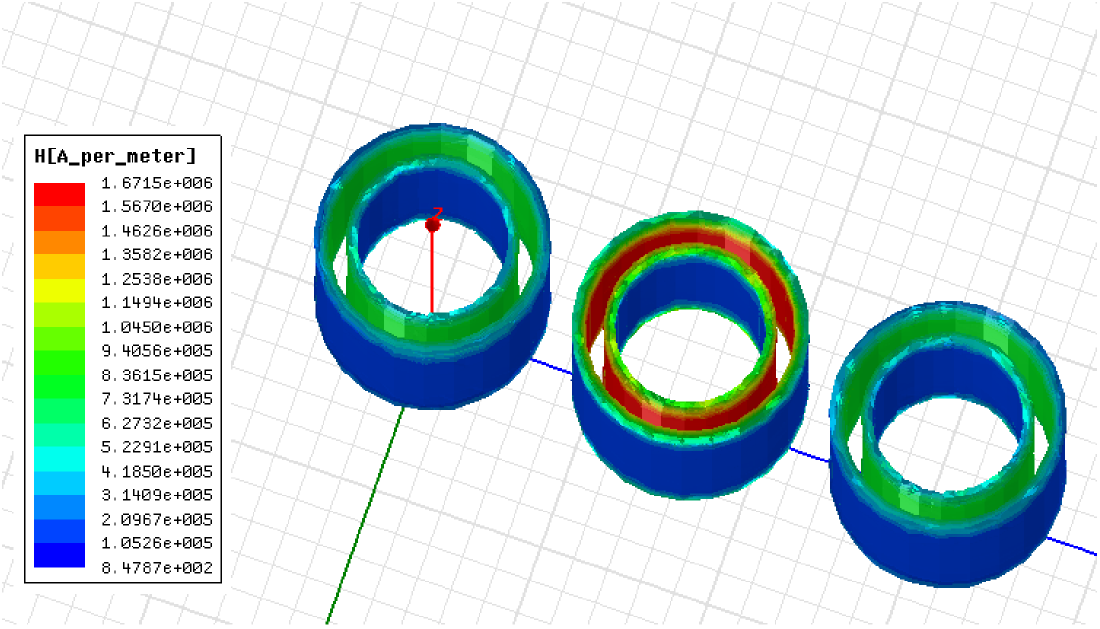

Figure 4.5 : Magnetic field intensity around cylindrical design windings.

In figure 4.6, volume force density distribution on low voltage windings of cylindrical design transformer under short circuit condition is given. Highest force density is on the center limb. This highest value, 2,0639 x 10^8 N/m^3, is the volume force density on the outer shell of low voltage winding of center limb. The average volume force density is 1,03195 x 10^8 N/m^3, which is the half of the outer shell force density. Total force on low voltage winding of center limb obtained by Maxwell software is:

F_{total} = (volume force density) x winding thickness x winding height

F_{total} = (1,03195 x 10^8 N/m^3) · (0,01616 m) · (0,505 m)

F_{total} = 842.153,76 N

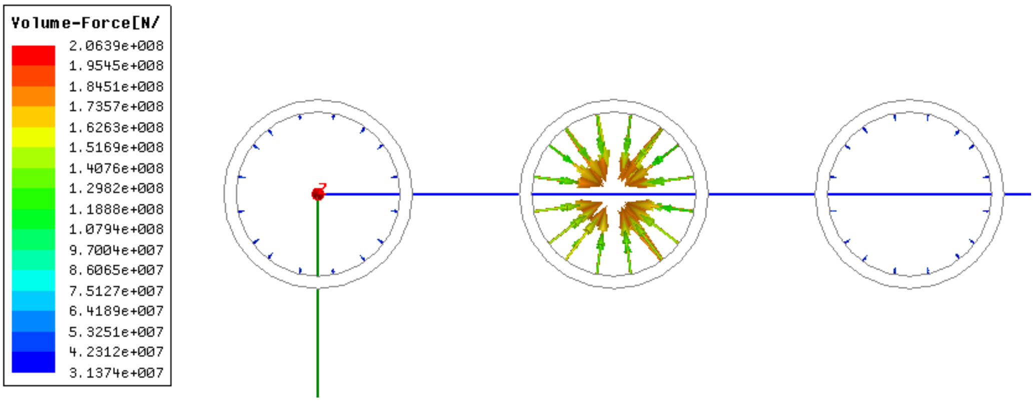

Figure 4.6 : Volume force density on cylindrical design LV windings.

A two-dimensional simulation of same transformer under same short circuit conditions is performed on FEMM software. When depth is defined 1 mm, force on low voltage winding is 799,611 N as given on figure 4.7. Multiplying this force with average winding circumference, total force on winding is obtained.

$F_{total} = (799{,}611\ N/mm) \cdot (\pi \cdot 0{,}317\ m)$

$F_{total} = 796.320{,}50\ N$

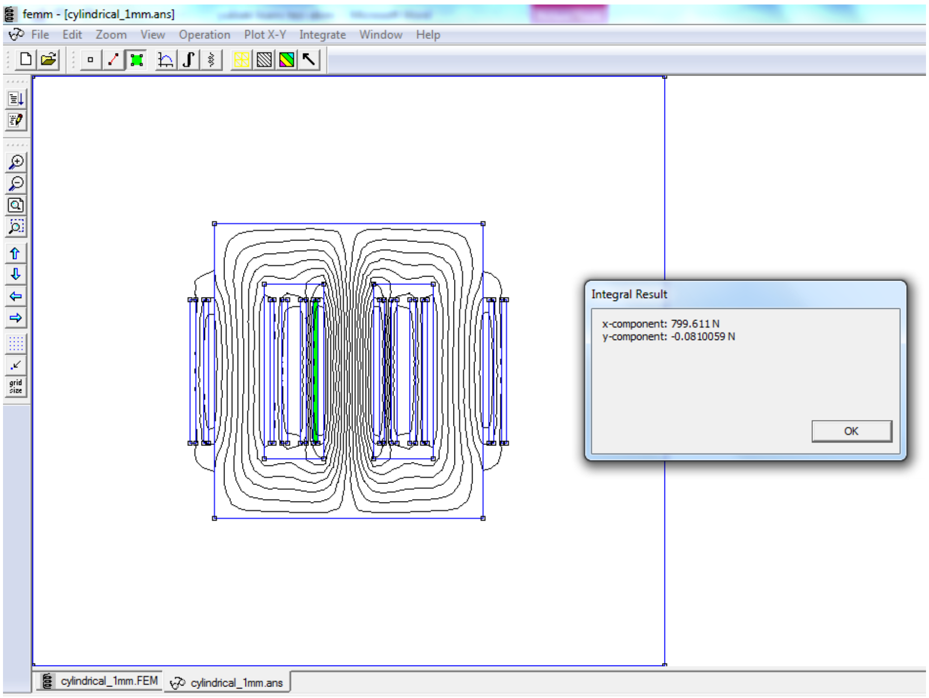

Figure 4.7 : Output of FEMM software.

Total force on low voltage winding is calculated at part 4.1 and at this part, the force is obtained by two different simulation software products. After being sure the results on table 4.2 are close, remaining results will be obtained by three-dimensional simulation in order to see not only the total values but also the distribution on structure.

Table 4.2 : Total force on low voltage winding under short circuit.

Method	Total force (N)
Analytical calculation	868.563,31
Maxwell software	842.153,76
FEMM software	796.320,50

Volume force density distribution on high voltage windings is given on figure 4.8.

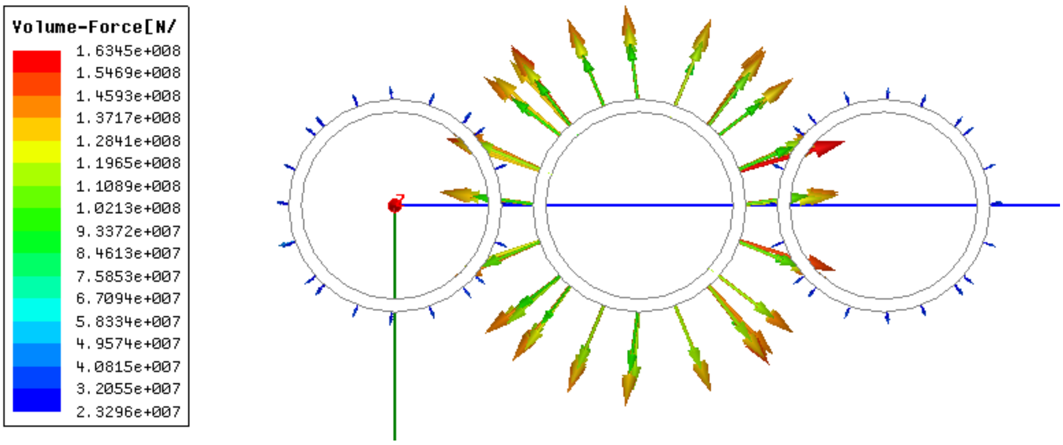

Figure 4.8 : Volume force density on cylindrical design HV windings.

4.2.2 Calculation for elliptical windings

Three-dimensional drawing including core, windings, lower and upper wooden supports and insulation rods between high voltage and low voltage windings for elliptical design transformer is given on figure 4.9. Figure 4.10 shows the simplified version of the same drawing for electromagnetic simulation.

Magnetic flux density around low voltage and high voltage windings is given on figure 4.11.

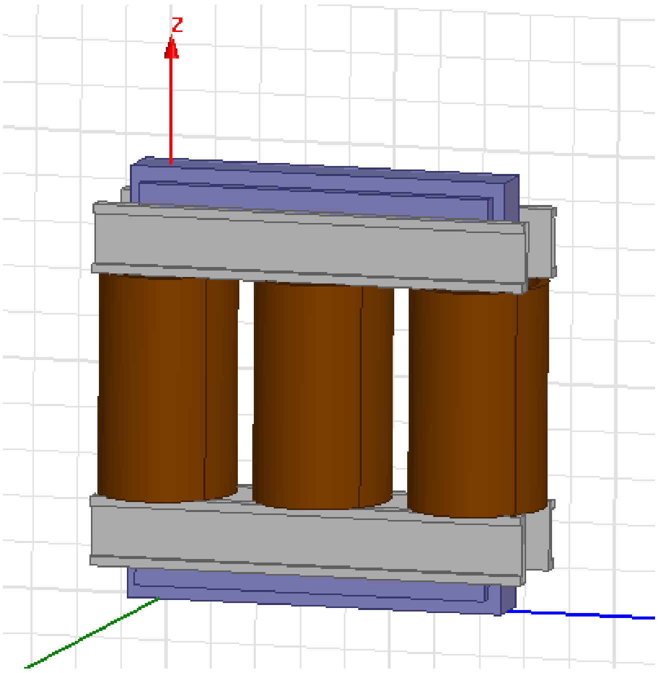

Figure 4.9 : Entire active part of elliptical design.

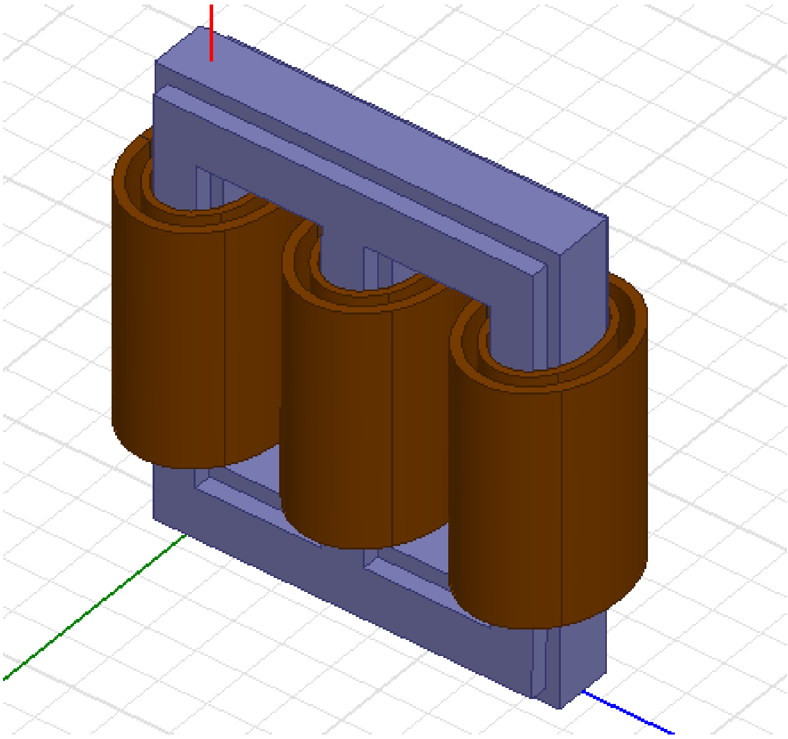

Figure 4.10 : Simplified version of elliptical design.

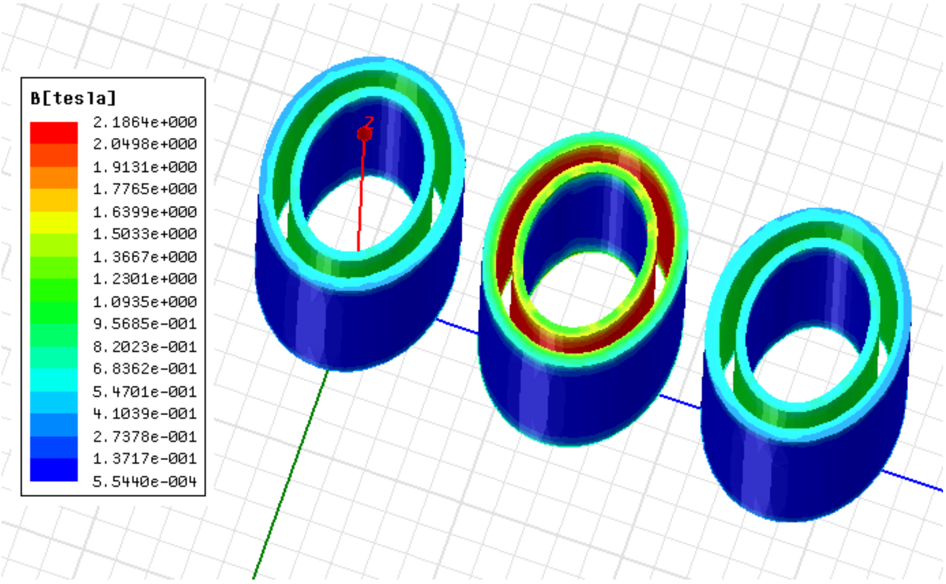

Figure 4.11 : Magnetic flux density around elliptical design windings.

Magnetic flux density for low voltage windings is given on figure 4.12. Like cylindrical design, flux density is almost constant along z-axis. Additionally, magnetic field intensity distribution is given on figure 4.13.

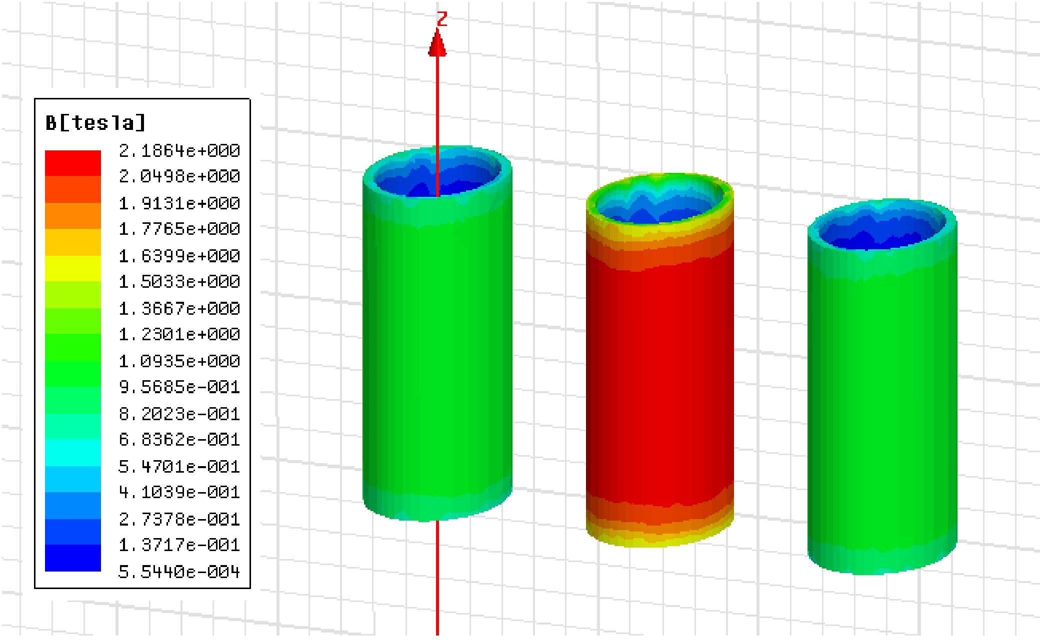

Figure 4.12 : Magnetic flux density on elliptical design LV windings.

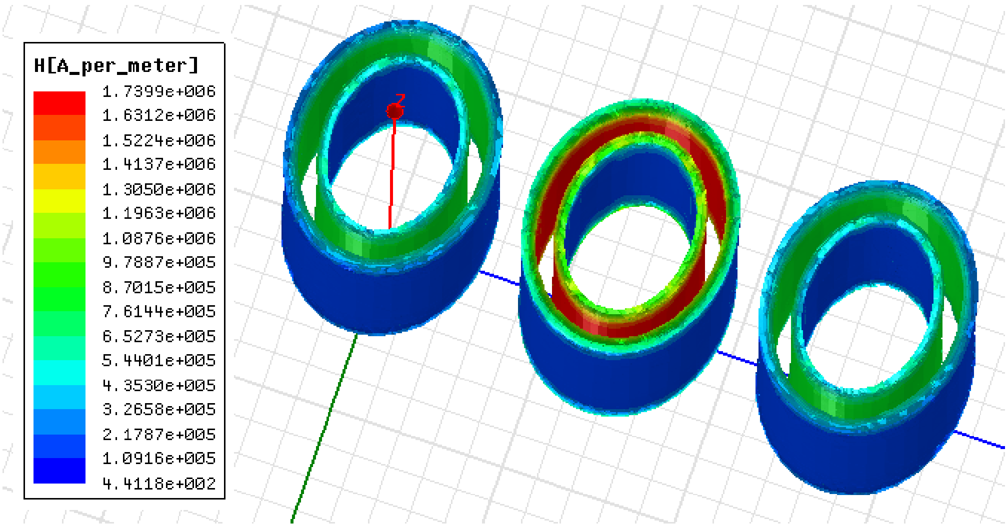

Figure 4.13 : Magnetic field intensity around elliptical design windings.

It is known that forces on narrow and wide portions of elliptical windings are not same. In order to observe this and obtain more accurate results, each winding is divided into four pieces. Two pieces are equivalent narrow pieces and remaining two ones are equivalent wide pieces. Each piece covers 90 degrees. Top view of force density distribution acting on low voltage winding is given on figure 4.14.

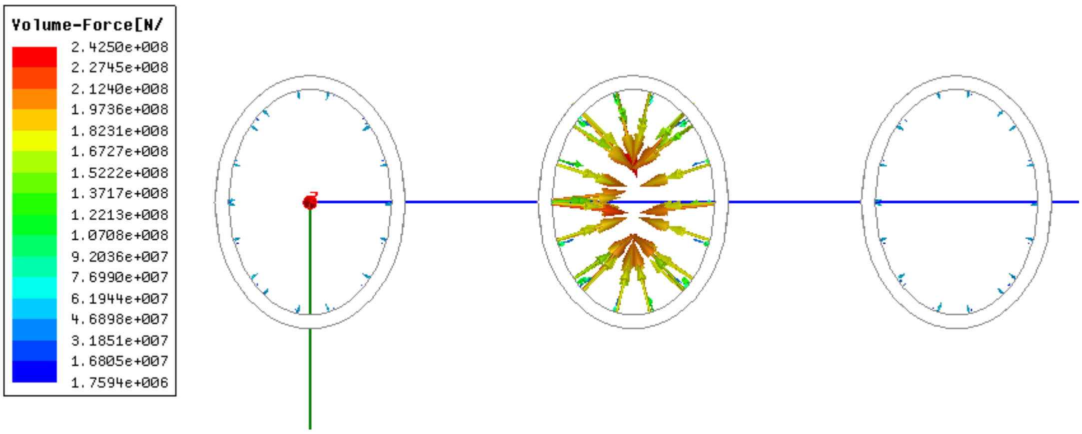

Figure 4.14 : Volume force density on elliptical design LV windings.

The chart on the left end of figure 4.14 gives the lower and upper values of force density. Since the forces on wide and narrow pieces are not equal, simulation results for each piece is obtained separately and force densities are read from the chart. Table 4.3 gives the force distribution of pieces for low voltage windings.

Table 4.3 : Force densities of low voltage winding pieces of elliptical design.

Limb	Piece	Force density (N/m^3)
End	Narrow	5,4528 x 10^7
End	Wide	6,1186 x 10^7
Center	Narrow	2,1798 x 10^8
Center	Wide	2,4250 x 10^8

Figure 4.15 shows the force density distribution for high voltage windings.

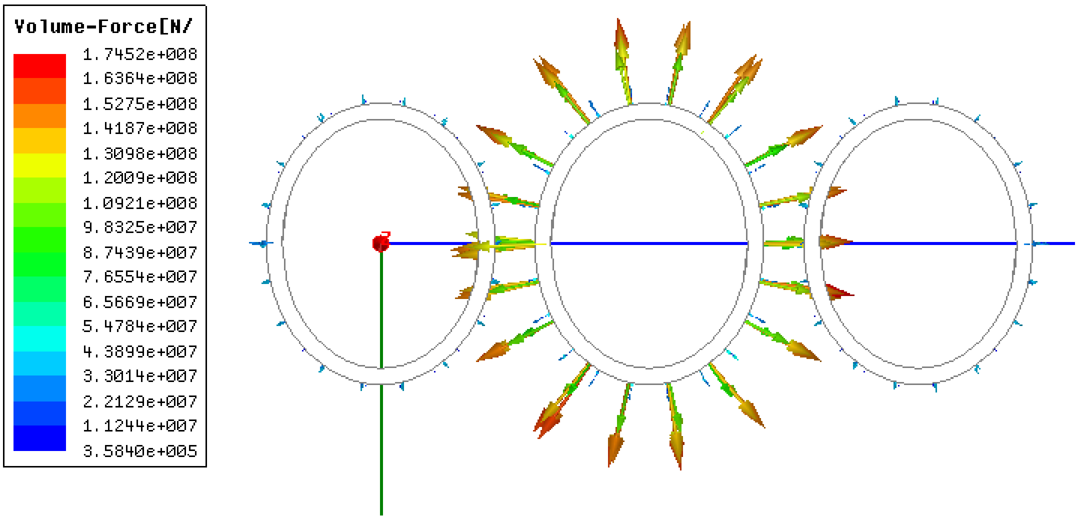

Figure 4.15 : Volume force density on cylindrical design HV windings.

Similar procedure is applied for high voltage windings and force distribution results for pieces are given on table 4.4.

Table 4.4 : Force densities of high voltage winding pieces of elliptical design.

Limb	Piece	Force density (N/m^3)
End	Narrow	3,9154 x 10^7
End	Wide	4,2244 x 10^7
Center	Narrow	1,5992 x 10^8
Center	Wide	1,7452 x 10^8

4.2.3 Calculation for square windings

The entire three-dimensional drawing including of square design is given on figure 4.16. Figure 4.17 shows the simplified version of the same drawing for electromagnetic simulation.

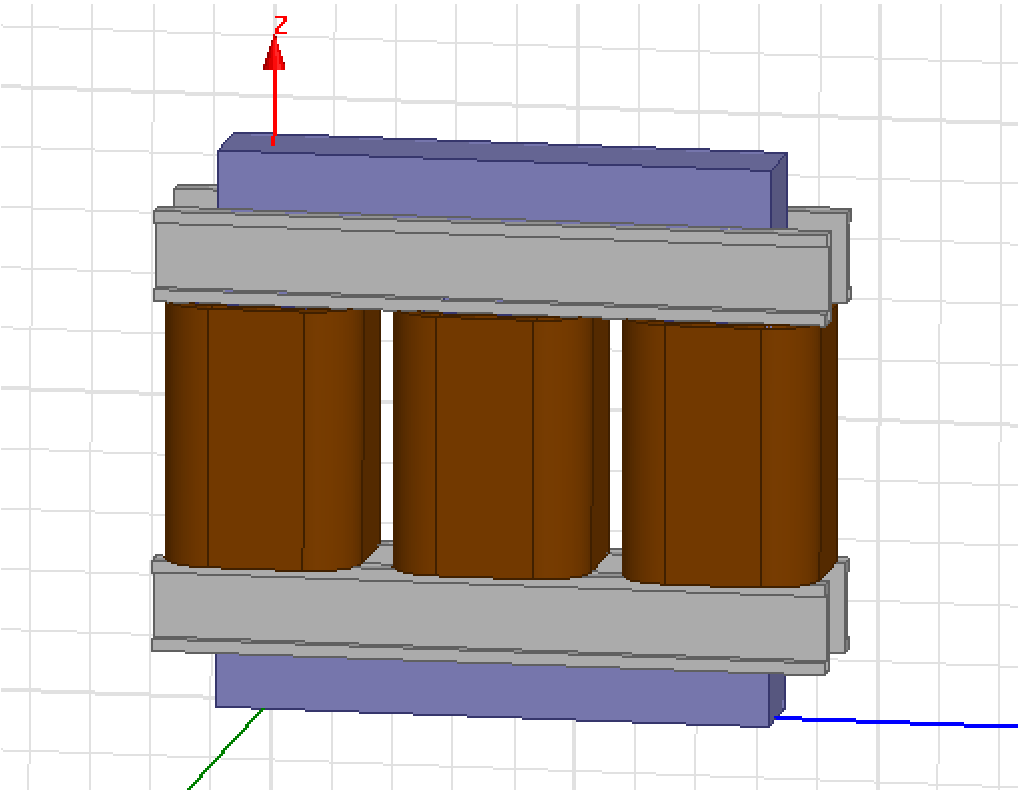

Figure 4.16 : Entire active part of square design.

Magnetic flux density around low voltage and high voltage windings is given on figure 4.18.

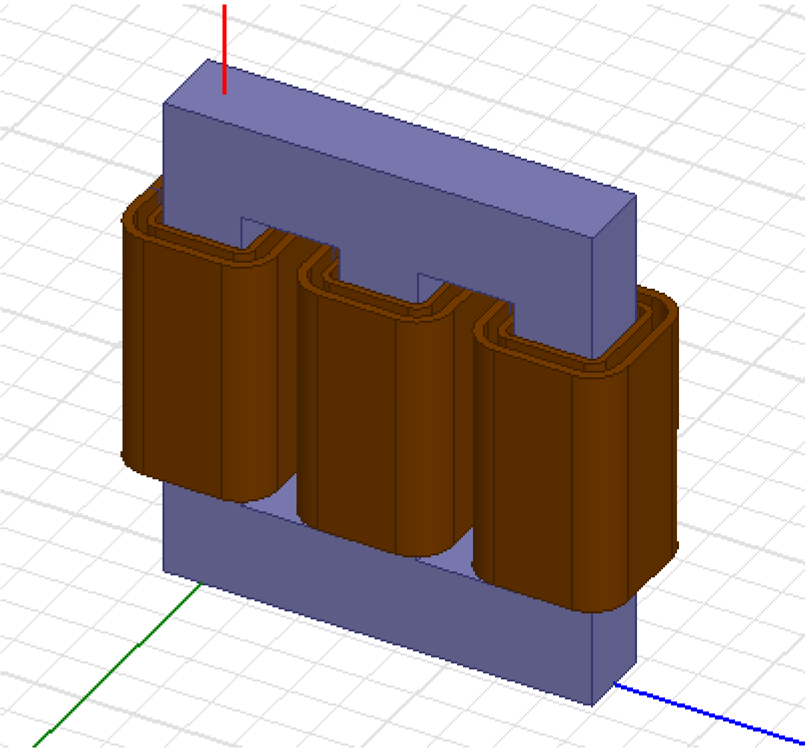

Figure 4.17 : Simplified version of square design.

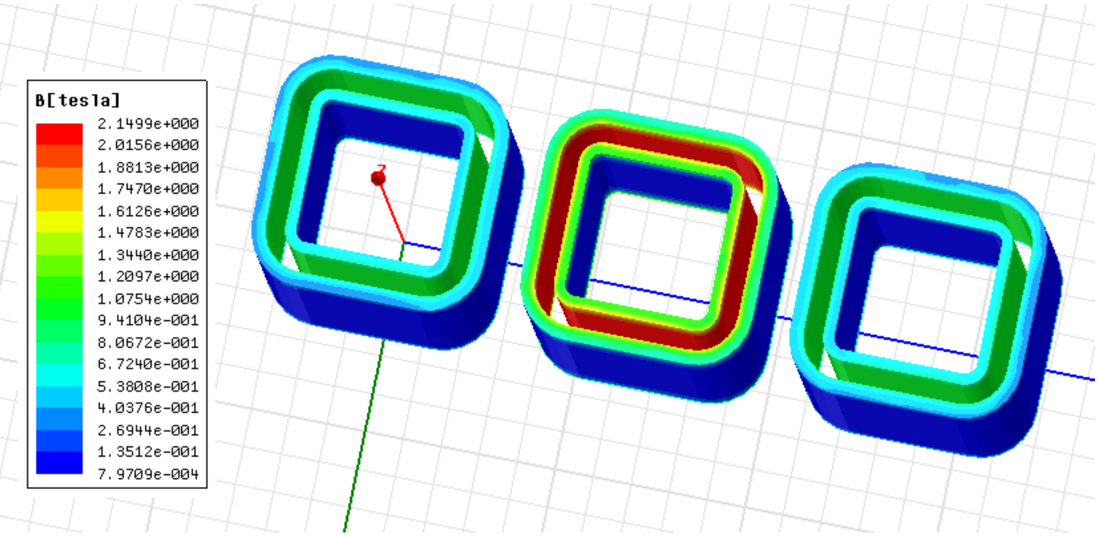

Figure 4.18 : Magnetic flux density around square design HV and LV windings.

Magnetic flux density for low voltage windings is given on figure 4.19. Like cylindrical and elliptical design, flux density is almost constant along z-axis. Additionally, magnetic field intensity distribution is given on figure 4.20.

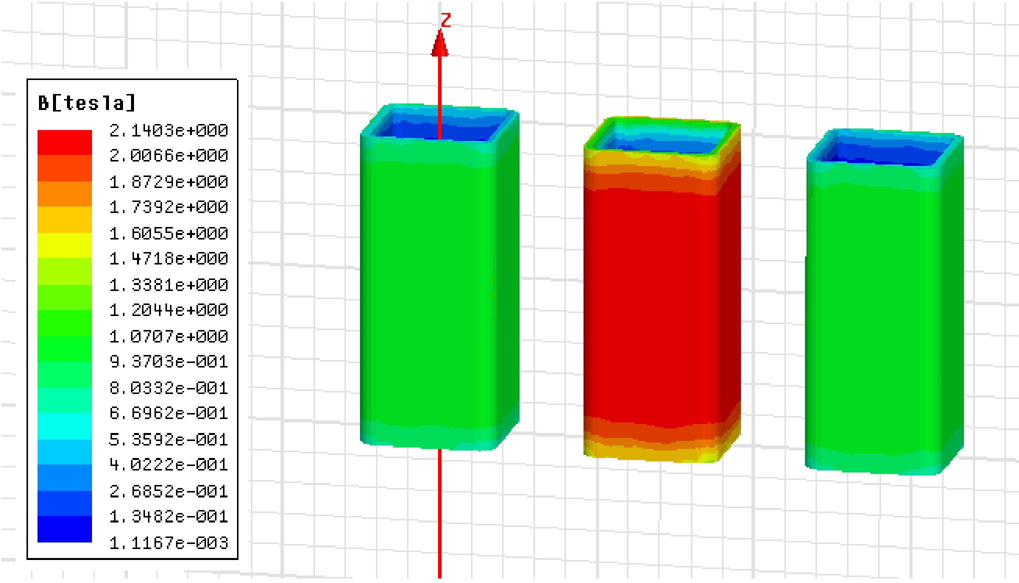

Figure 4.19 : Magnetic flux density on square design LV windings.

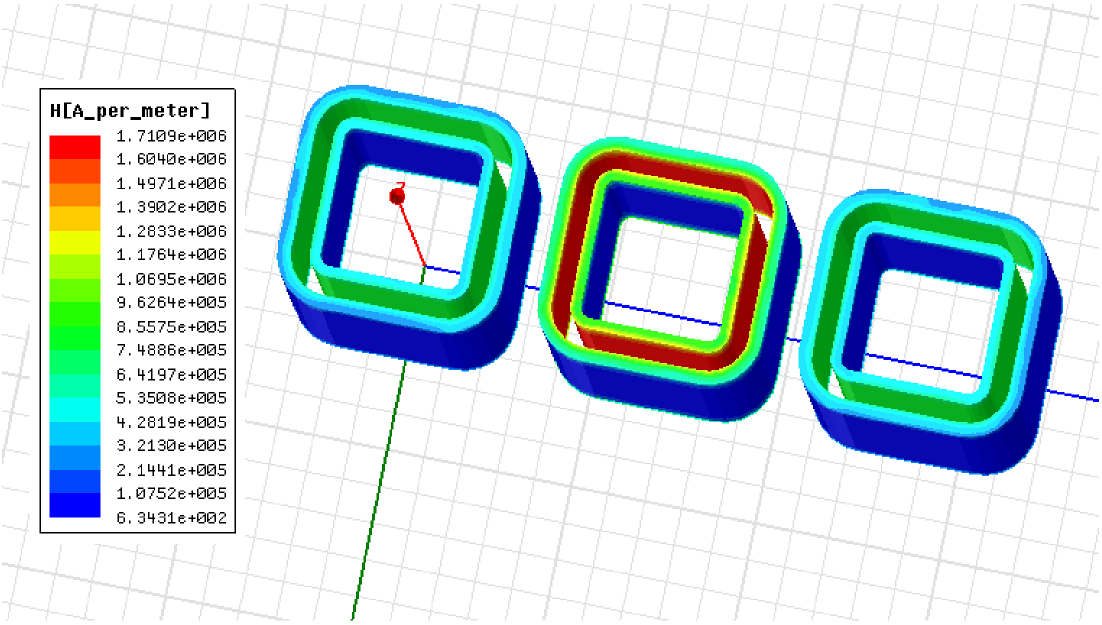

Figure 4.20 : Magnetic field intensity around square design windings.

Like elliptical design, forces on windings are not uniformly distributed on each winding in square design. Force distribution on corner and flat portions of square windings are different. In order to observe this and obtain more accurate results, each winding is divided into eight pieces. Four pieces are equivalent corner pieces and remaining four ones are equivalent flat pieces. Top view of force density distribution acting on low voltage winding is given on figure 4.21.

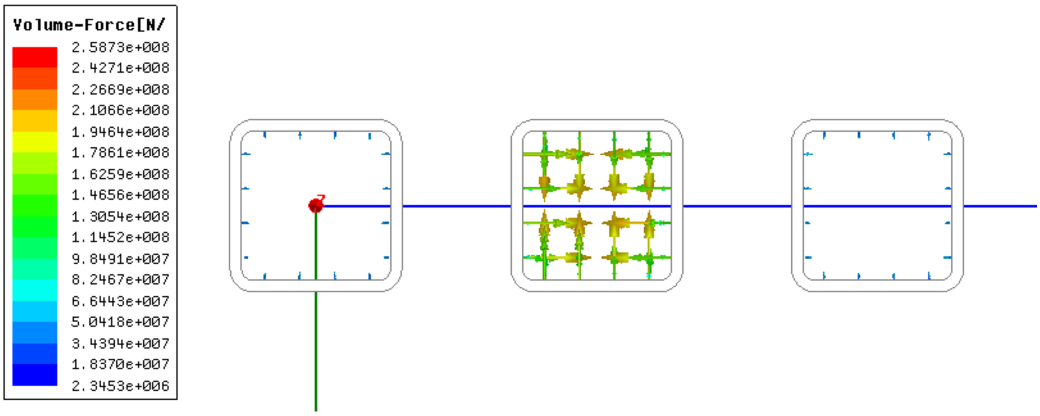

Figure 4.21 : Volume force density on square design LV windings.

The chart on the left end of figure 4.21 gives the lower and upper values of force density like charts given before. Since the forces on corner and flat pieces are not equal, same procedure like elliptical design simulation is followed and simulation results for each piece are obtained separately. Force densities are read from the chart and force distribution of pieces for low voltage windings are given on table 4.5.

Table 4.5 : Force densities of low voltage winding pieces of square design.

Limb	Piece	Force density (N/m^3)
End	Flat	5,5303 x 10^7
End	Corner	6,2899 x 10^7
Center	Flat	2,1257 x 10^8
Center	Corner	2,5873 x 10^8

Figure 4.22 shows the force density distribution for high voltage windings.

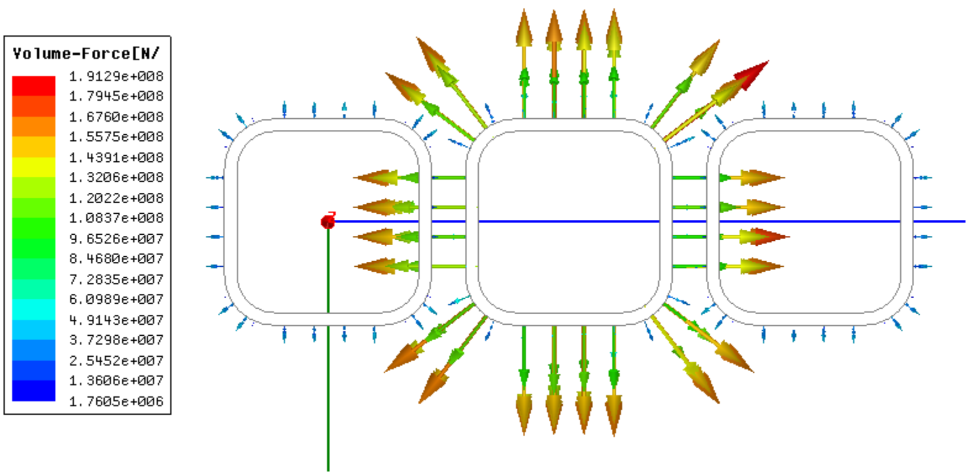

Figure 4.22 : Volume force density on square design HV windings.

Similar procedure is applied for high voltage windings and force distribution results for pieces are given on table 4.6.

Table 4.6 : Force densities of high voltage winding pieces of square design.

Limb	Piece	Force density (N/m^3)
End	Flat	4,0214 x 10^7
End	Corner	4,6623 x 10^7
Center	Flat	1,6830 x 10^8
Center	Corner	1,9129 x 10^8

4.3 Comparison of Force Density Distributions

Volume force density values in N/mm^3 for three types of transformers are given on table 4.7.

Table 4.7 : Volume force densities on regions of windings under short circuit.

Volume Force Density (N/mm^3)							
Center limb				End limbs			
Cylindrical				Cylindrical			
LV		HV		LV		HV	
0,20639		0,16345		0,049515		0,042097	
Elliptical				Elliptical			
LV narrow	LV wide	HV narrow	HV wide	LV narrow	LV wide	HV narrow	HV wide
0,21798	0,24250	0,15992	0,17452	0,054528	0,061186	0,039154	0,042244
Square				Square			
LV flat	LV corner	HV flat	HV corner	LV flat	LV corner	HV flat	HV corner
0,21257	0,25873	0,16830	0,19129	0,055303	0,062899	0,040214	0,046623

Comparing LV and HV forces per mm^3 on table for each design and for each region of structure, it is observed that results of LV windings are higher than results of HV windings. Since total net force on both LV and HV windings of one limb should be zero, total bending force on LV winding for one design is equal to that on HV winding with reverse direction. The difference between forces per mm^3 is mainly because of coil diameters and thicknesses. During construction, LV windings are assembled on core. Later, wooden insulators form oil gap and then, HV windings are assembled. This causes high voltage windings having higher coil diameters than low voltage windings. Additionally, LV windings have rectangular cross-sections while HV windings have circular cross-sections. This causes higher thickness and higher average diameter for high voltage windings. Moreover, insulation paper around copper is more in high voltage coils since there are more turns. These makes high voltage windings having larger dimensions comparing to low voltage windings and thus having less force per mm^3 although winding heights are equal.

In elliptical and square design, different regions of same structure have different results as expected. Wider parts of elliptical windings are under higher volume force densities comparing to the narrow parts of same windings. Similarly, corners of square windings are under higher volume force densities comparing to the flat parts.

Force densities for square design are high. Especially, it is observed that corners of square design windings are under high volume force density comparing with the remaining regions of all three designs. Additionally, elliptical windings are under higher volume force densities comparing with those of cylindrical design. It can be seen that windings of square design transformer are subjected to highest force densities among three designs while those of cylindrical design transformer are subjected to lowest ones under short circuit conditions.

5. MECHANICAL SIMULATION AND DEFORMATIONS

In this part, the impact of short circuit forces on transformer structures is analyzed. In order to achieve this, mechanical simulation software, ANSYS, is utilized. For three types of transformers designed before, forces obtained by electromagnetic simulation are applied to related parts of transformers respectively. The short circuit test is simulated according to the IEC standards [14].

5.1 Force to Pressure Transformation

Volume force densities were obtained by electromagnetic simulation before. The force densities were those on outer shell of low voltage windings and inner shell of high voltage windings. To apply these forces to the structures, forces are converted to pressure. The force densities obtained are multiplied by the thicknesses of the windings to obtain pressures in N/mm^2, which is equal to MegaPascal (MPa). Additionally, average pressure on windings is obtained by taking the half of the obtained values. The pressure values obtained by multiplication of average force densities and winding thicknesses are given on table 5.1.

Table 5.1 : Pressure on parts of winding shells under short circuit.

Pressure (Mpa = N/mm^2)							
Center limb				End limbs			
Cylindrical				Cylindrical			
LV		HV		LV		HV	
1,6676		1,6533		0,4001		0,4258	
Elliptical				Elliptical			
LV narrow	LV wide	HV narrow	HV wide	LV narrow	LV wide	HV narrow	HV wide
1,6076	1,7884	1,6320	1,7810	0,4021	0,4512	0,3996	0,4311
Square				Square			
LV flat	LV corner	HV flat	HV corner	LV flat	LV corner	HV flat	HV corner
1,5390	1,8732	1,5635	1,7771	0,4004	0,4554	0,3736	0,4331

5.2 Building the Simulation Structure

After getting the pressure values, the simulation structure can be created. For ANSYS simulation, Engineering Data, Geometry, Model parts are prepared respectively.

5.2.1 Material properties

At Engineering Data part, used materials are selected and rearranged if necessary. For our study, steel, copper, wood and insulation paper are used since only the impact of short circuit on active part is analyzed. Material properties given on Table 5.2 are used at simulation [13].

Table 5.2 : Material properties.

Material	Structures	Elastisity (Mpa)	Density (g/cm^3)	Poisson Ratio	Yield Strength (Mpa)
Steel	Core	110.000	7,2	0,3	NA
Copper	Windings	750	8,9	0,3	120
Wood	Isolation	16.000	1,3	0,3	100

5.2.2 Structure simplification

At Geometry part, three-dimensional drawings of designed transformers prepared before are used. For each transformer, the entire geometry can be constructed and the forces can be applied to it but applying following simplifications makes the analysis easier and faster:

- Three limbs of the transformer are identical since the same materials are used for the same geometries. For the worst-case analysis, it is enough to analyze only center limb where the maximum forces are formed.
- The analysis is done in order to observe the impact of short circuits on transformer windings. Remaining parts are assumed to be fixed.

5.2.3 Time varying pressure

Current variation by time was given in equation **2.24** and force expression was given in equation **2.30**. Resistances and equivalent inductances are given on table 5.3.

Since the relation between pressure and force is linear, pressure has similar time varying characteristics with force on windings.

Table 5.3 : Equivalent resistances and inductances.

Cylindrical	
L_{eq} (H)	R_{eq} (ohm)
1,84	196,52
Elliptical	
L_{eq} (H)	R_{eq} (ohm)
1,69	186,94
Square	
L_{eq} (H)	R_{eq} (ohm)
1,71	201,91

Force on transformer windings is proportional to the square of the current. Maximum force densities obtained at part 4 are the force densities when the short circuit takes place at time instant, which makes initial current maximum. Since other variables are fixed in time, the square of the ratio between instant current and initial (which is also maximum) current is the ratio between instant pressure on windings to the maximum pressure. The time dependent pressure on windings is

$$P(t) = 0{,}25 \cdot P_{\max} \left[\sin(wt + \alpha - \theta) + e^{-\frac{Rt}{L}} \sin(\alpha - \theta) \right]^2 \quad \textbf{(5.1)}$$

Figure 5.1 shows the change in average pressure on low voltage winding of center limb of cylindrical winding transformer between $t = 0$ and $t = 0{,}1$ seconds for $\alpha - \theta = -\pi/2$.

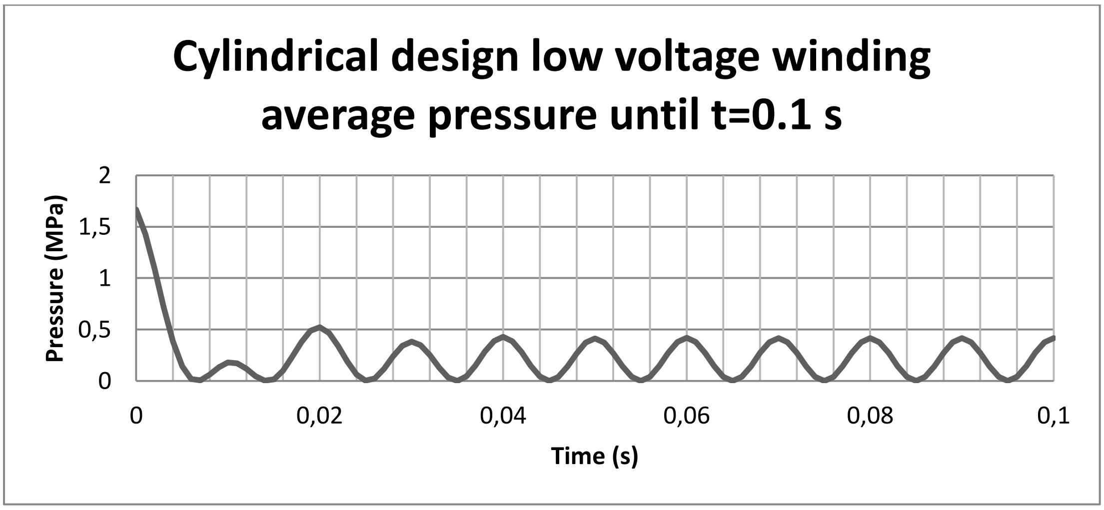

Figure 5.1 : Pressure on LV winding of center limb.

Since the short circuit test duration is 0,5 seconds for subject transformers, the pressure will be applied on the windings until $t = 0,5$ seconds. As seen on figure 5.1, the effect of exponential part in pressure is invisible after $t = 0,08$ sec. On the other hand, the sinusoidal pressure continues until $t = 0,5$ seconds with double line frequency. Pressure variations for remaining parts of three types of transformers are similar with related peak values and time constants. Total simulation time is 1 sec. to observe the variation of outputs after the interruption of current. Pressures on structures are zero between $t = 0,5$ and $t = 1$ sec.

5.3 Simulation Results

Deformation and Equivalent (von-Mises) Stress on structures are obtained by simulation. Results for three designs are given on figures 5.2 - 5.13. The green curves show the variation of maximum deformation or stress on the mentioned structure and the red curves show those of minimum ones.

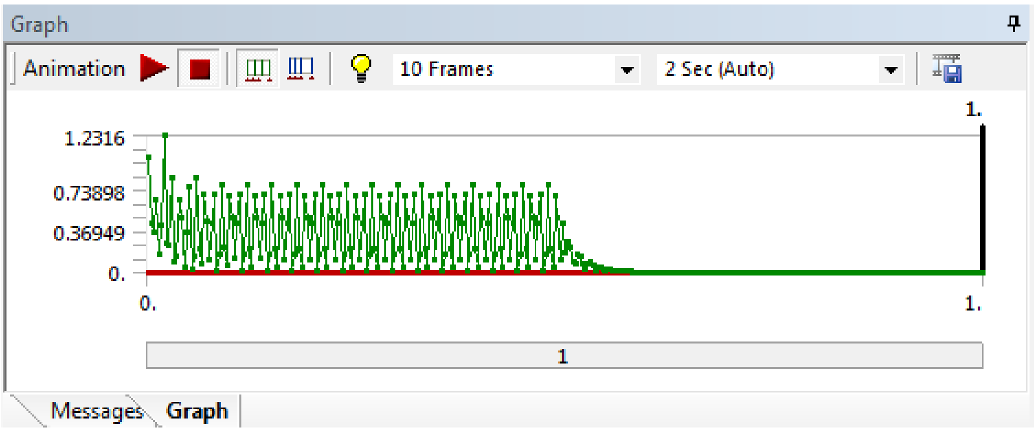

Figure 5.2 : Deformation on HV winding of cylindrical design.

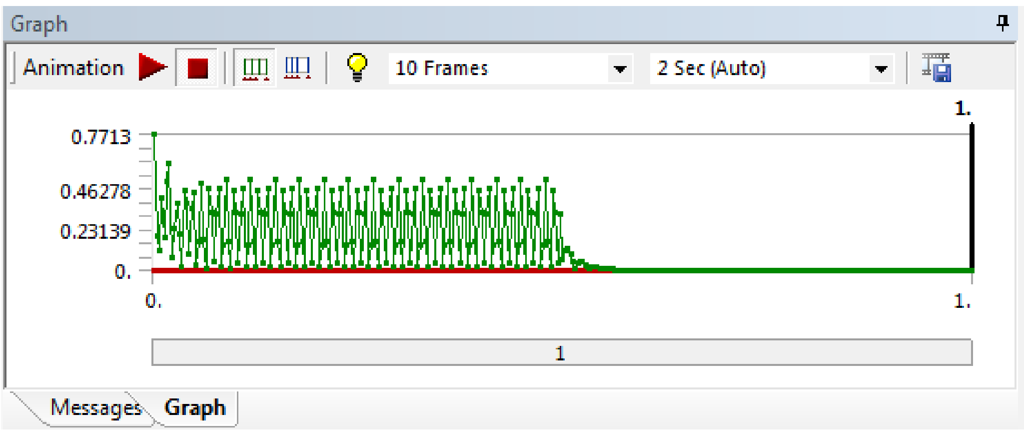

Figure 5.3 : Deformation on LV winding of cylindrical design.

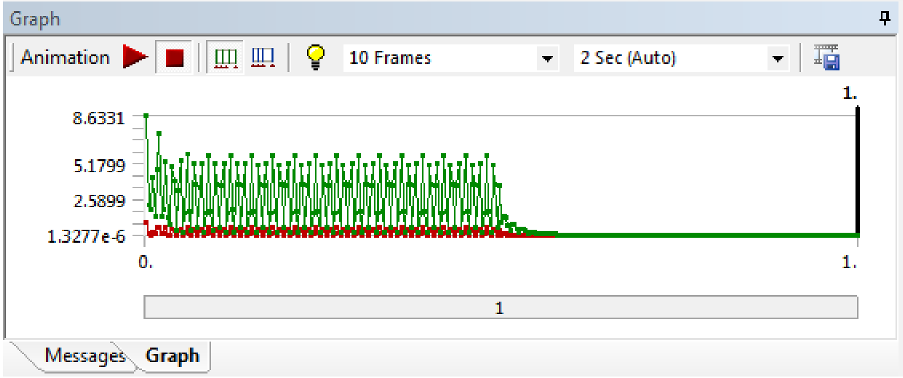

Figure 5.4 : Equivalent stress on HV winding of cylindrical design.

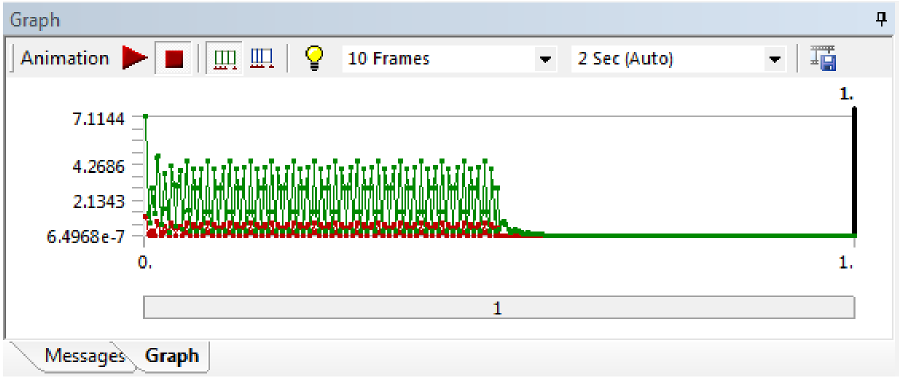

Figure 5.5 : Equivalent stress on LV winding of cylindrical design.

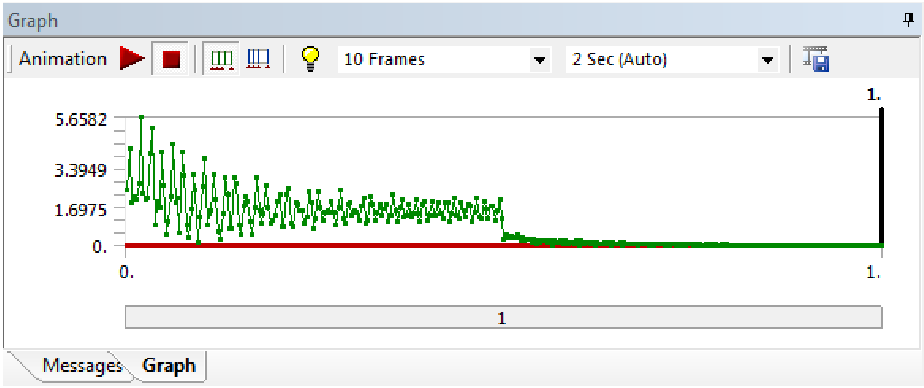

Figure 5.6 : Deformation on HV winding of elliptical design.

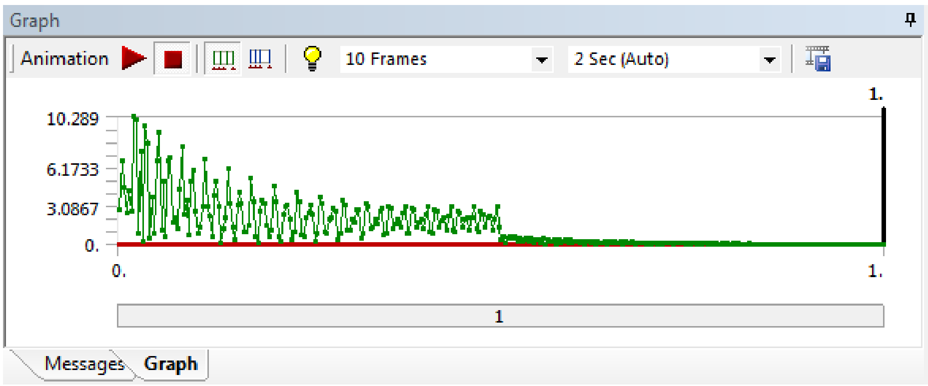

Figure 5.7 : Deformation on LV winding of elliptical design.

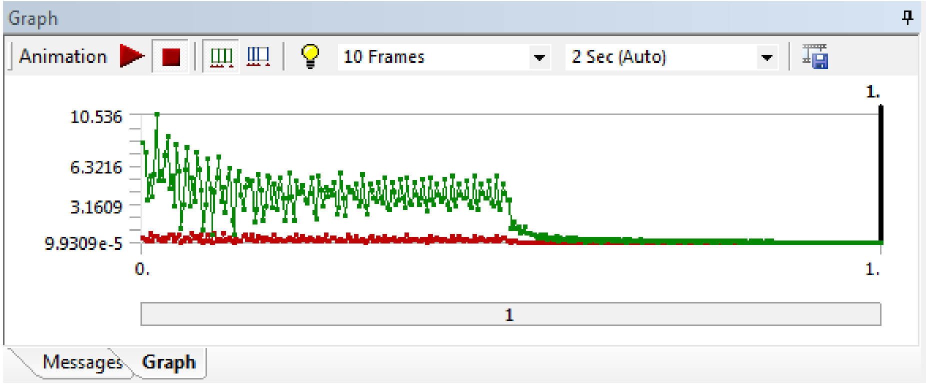

Figure 5.8 : Equivalent stress on HV winding of elliptical design.

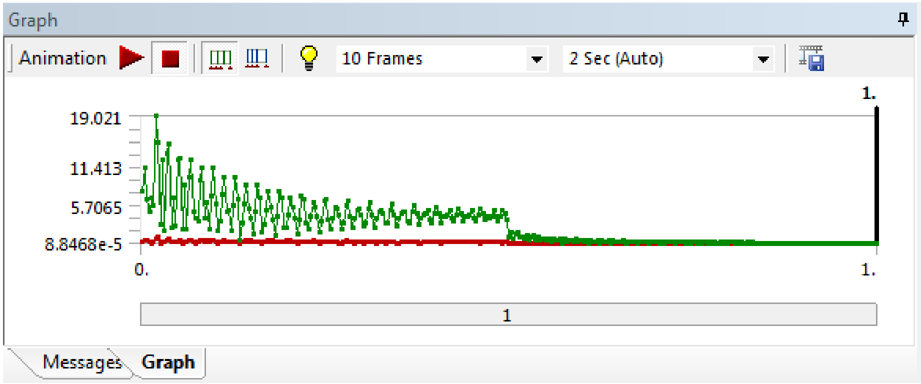

Figure 5.9 : Equivalent stress on LV winding of elliptical design.

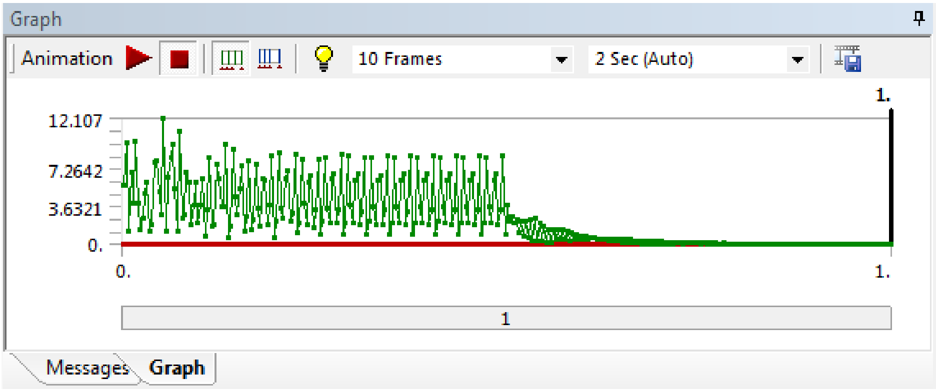

Figure 5.10 : Deformation on HV winding of square design.

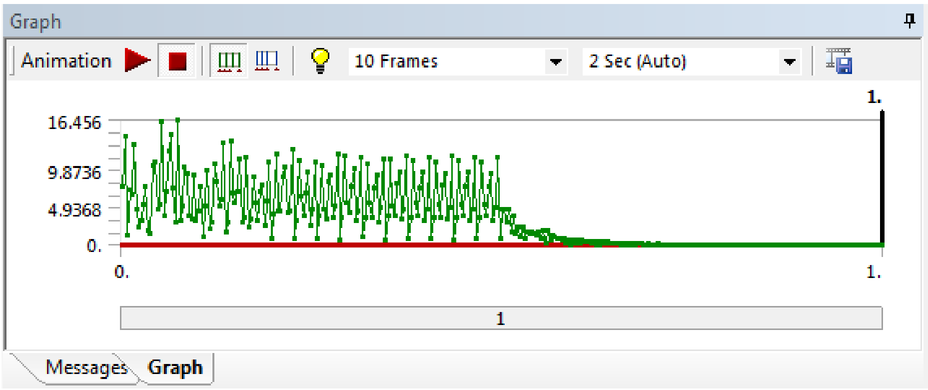

Figure 5.11 : Deformation on LV winding of square design.

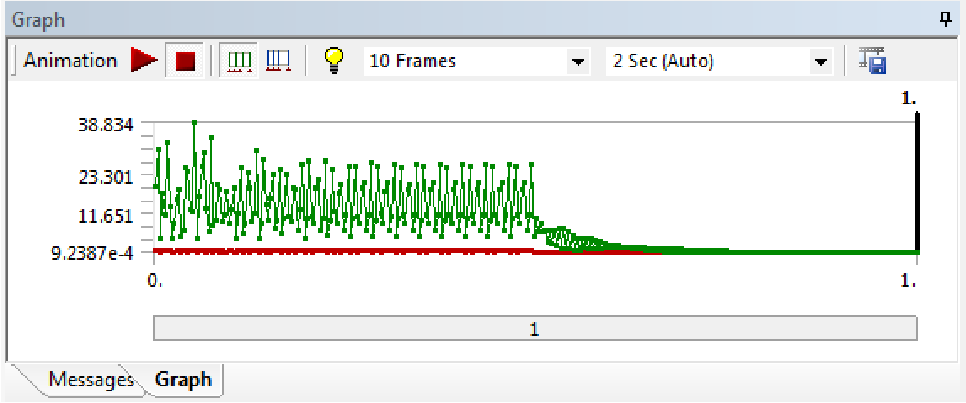

Figure 5.12 : Equivalent stress on HV winding of square design.

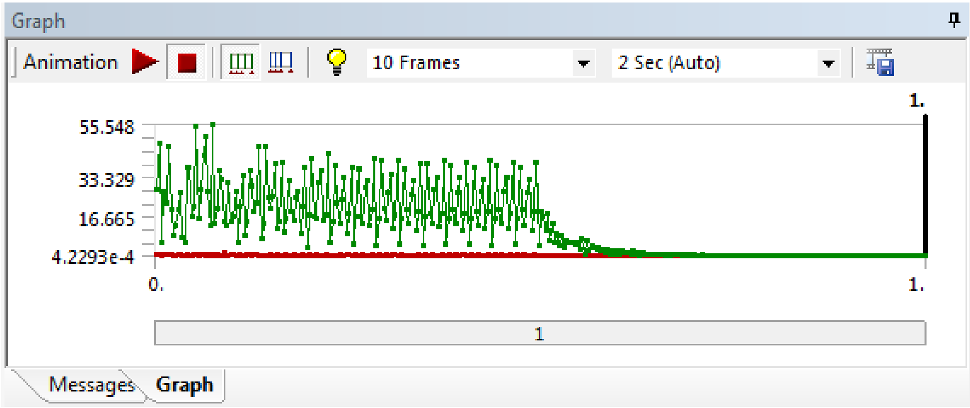

Figure 5.13 : Equivalent stress on LV winding of square design.

All deformation and equivalent stress variations in time are obtained. Maximum values for deformations and stresses for three designs are given on table 4.8.

Table 4.8 : Maximum deformation and stress on windings.

Maximum Deformation (mm)		Maximum Stress (Mpa)	
Cylindrical		Cylindrical	
HV	LV	HV	LV
1,2316	0,7713	8,6331	7,1144
Elliptical		Elliptical	
HV	LV	HV	LV
5,6582	10,289	10,536	19,021
Square		Square	
HV	LV	HV	LV
12,107	16,456	38,834	55,548

Maximum deformations on cylindrical windings are very low comparing to other designs. The highest deformations occur on square design as expected. Similarly, maximum stresses on cylindrical design windings are lowest while those on square windings are highest.

On figures 5.14 – 5.25, maximum deformations and stresses on structures are given on three-dimensional drawings.

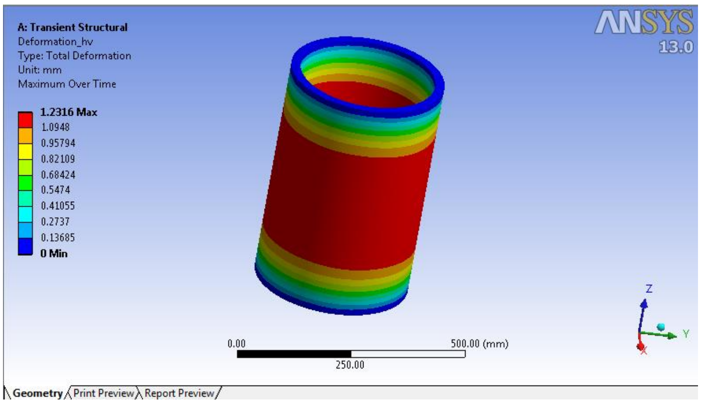

Figure 5.14 : Maximum deformation on HV winding of cylindrical design.

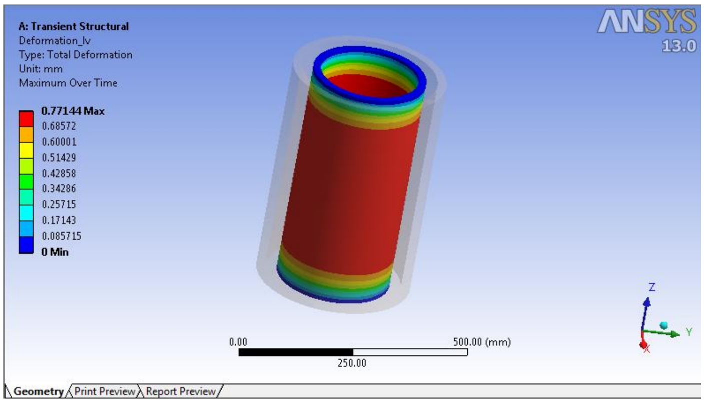

Figure 5.15 : Maximum deformation on LV winding of cylindrical design.

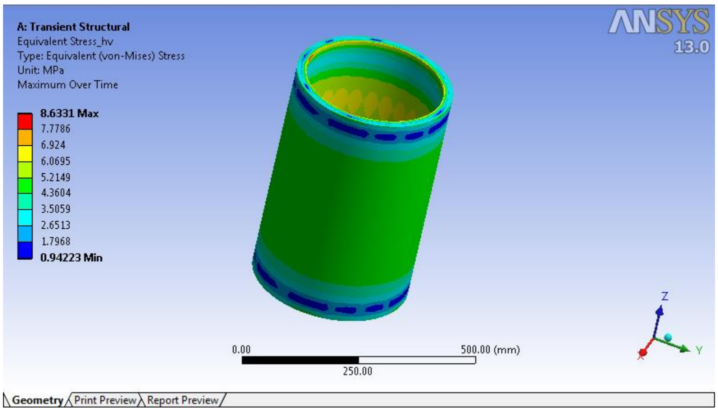

Figure 5.16 : Maximum stress on HV winding of cylindrical design.

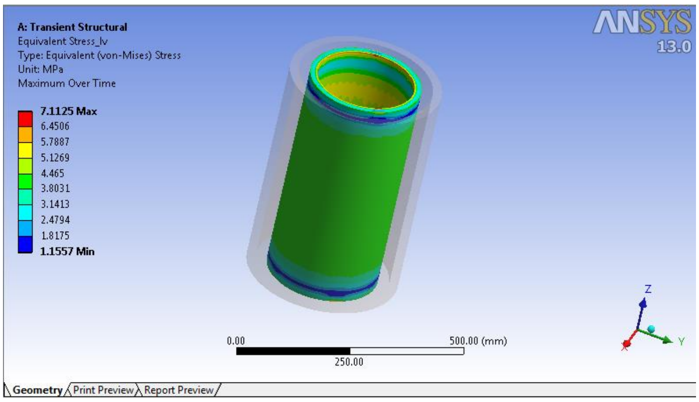

Figure 5.17 : Maximum stress on LV winding of cylindrical design.

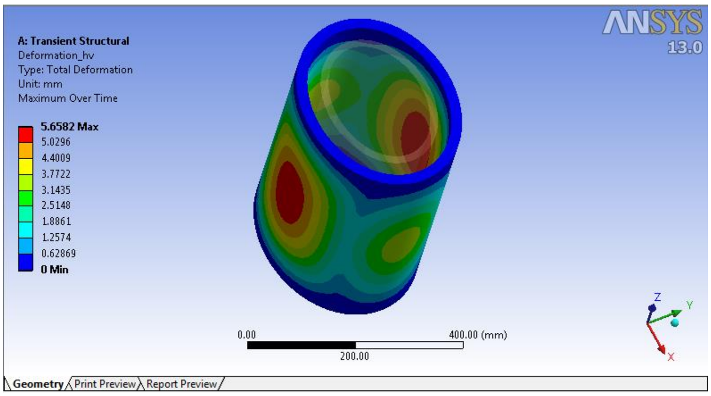

Figure 5.18 : Maximum deformation on HV winding of elliptical design.

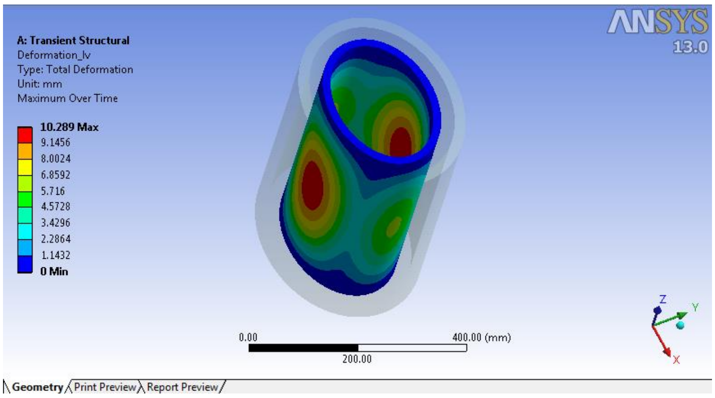

Figure 5.19 : Maximum deformation on LV winding of cylindrical design.

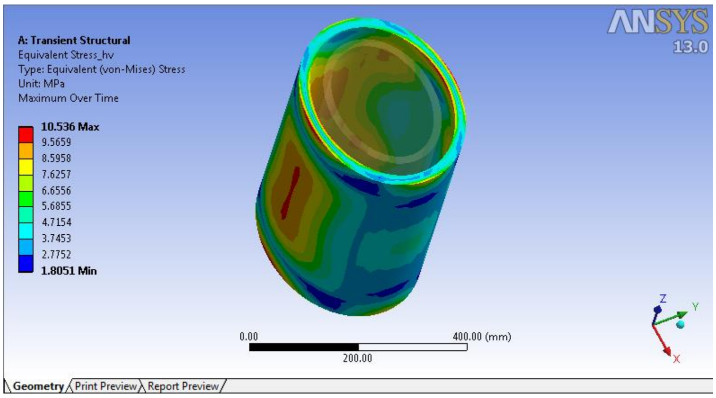

Figure 5.20 : Maximum stress on HV winding of elliptical design.

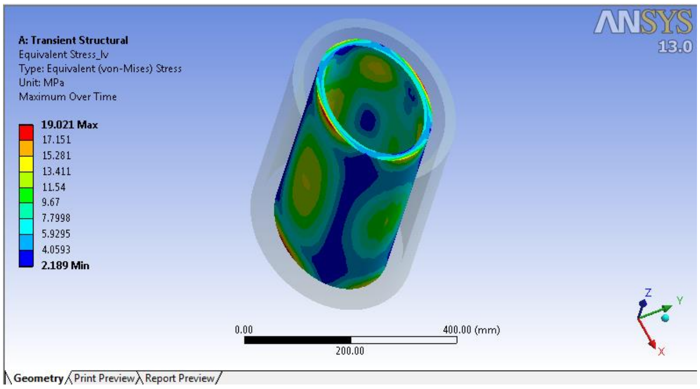

Figure 5.21 : Maximum stress on LV winding of elliptical design.

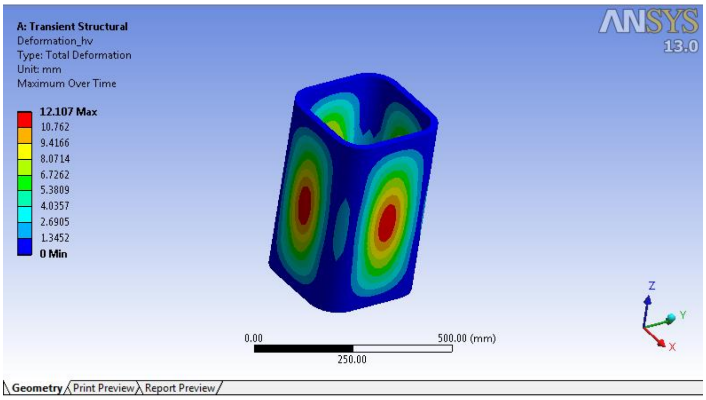

Figure 5.22 : Maximum deformation on HV winding of square design.

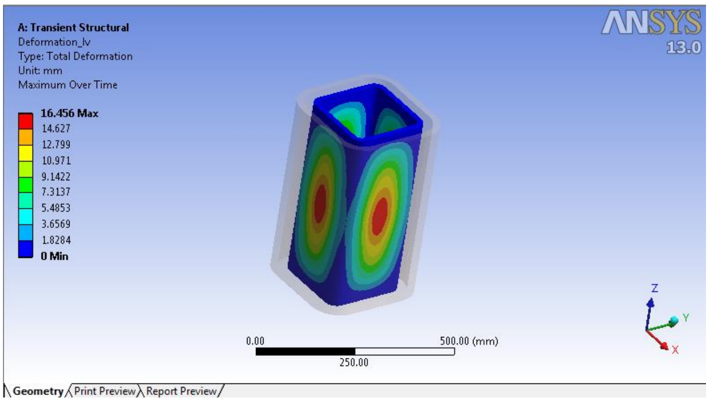

Figure 5.23 : Maximum deformation on LV winding of square design.

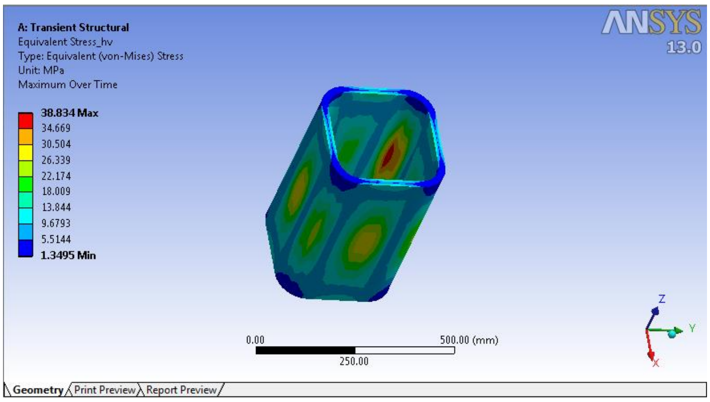

Figure 5.24 : Maximum stress on HV winding of square design.

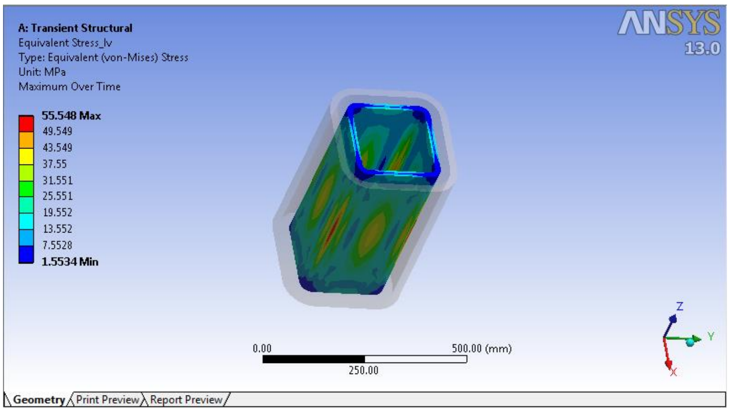

Figure 5.25 : Maximum stress on LV winding of square design.

6. CONCLUSIONS AND RECOMMENDATIONS

In this thesis, it was aimed to analyze the effect of winding geometry on short-circuit forces and to compare mechanical deformations caused by these forces for transformers having three different winding geometries under the same design constraints. In order to achieve this, three transformers in different winding geometries namely cylindrical, elliptical and square are designed where power rating, high voltage, low voltage, impedance, operation frequency, load power factor, losses, magnetic flux density, copper current density and core loss factor are all kept unchanged. For each design, all operational quantities, including electrical, mechanical and heating&cooling performance are checked basically for verification. Three-dimensional entire drawings including core, windings, insulation material and mechanical support equipment for three designs are prepared.

Using the time-varying short circuit current expression, short circuit instantaneous current for worst-case is calculated. Then, instantaneous forces created under short-circuit operations are calculated analytically. All designs are then analyzed by FEA (finite element analysis) using two different electromagnetic simulation commercial software, Maxwell and FEMM. Magnetic and electrical quantities and mechanical force are obtained. It is shown that forces on windings obtained by Maxwell, FEMM and analytical calculation are close. After comparison, Maxwell software is utilized in order to obtain remaining forces and force distributions on different regions of windings.

Electromagnetic simulation results show that LV windings are subjected to higher forces per m^3 than HV windings for all designs and all regions of structures. Additionally, volume force densities on wider parts of elliptical windings are higher than narrow parts of same windings. Similarly, corners of square windings are under higher volume force densities comparing to the flat parts. Among three designs, force densities for square design are high. Especially, it is observed that corners of square design windings are under high volume force density comparing with the remaining regions of all three designs. Additionally, elliptical windings are under higher volume force densities comparing with those of cylindrical design. It is proven that square design transformer windings are subjected to highest force densities among three designs while those of cylindrical design transformer are subjected to lowest ones under short circuit conditions.

The impact of short circuit forces on transformer windings is simulated by mechanical simulation software, ANSYS. Using the volume force densities, equivalent peak pressure values are obtained for all regions of three designs. Additionally, time varying pressures are generated using electrical time constants of each transformer for mechanical simulation. After selecting used materials, rearranging the material properties and simplifying the structures, mechanical simulation is finalized for three designs. According to the mechanical simulation results, maximum deformations on cylindrical windings are very low comparing to other designs. It is seen that the highest deformations occur on square design as expected. Similarly, maximum stresses on cylindrical design windings are lowest while those on square windings are highest.

The transformer analyzed in this study is a distribution transformer commonly used in electrical power system. First, design for different geometries is done and then, electromagnetic and mechanical analysis for each design is finalized in order to obtain forces, deformation and stresses on structures under short circuit. The steps followed in this study can be applied for all power and distribution transformers by manufacturers before the manufacturing process begins in order to monitor the effects of possible short circuits on transformer structure. Thanks to this, revisions can be made on design if the short circuit forces, stresses and deformations are over the limited levels. Additionally, this study show that the most desired results are obtained when the windings are cylindrical and if the geometry is changed for some reasons, strength of transformer should be checked by calculation or simulation in order to be sure the transformer withstands short circuits.

REFERENCES

[1] **Kulkarni, S. V. and Khaparde, S. A.** (2004). Transformer Engineering Design and Practice. Mumbai : Indian Institute of Technology.

[2] **Boduroğlu, T.** (1982). Elektrik Makinaları Dersleri: Teori, Hesap, Konstrüksiyon c.1. İstanbul : İTÜ.

[3] **Bharat Heavy Electricals Limited.** (2005). Transformers. New York : Mc-Graw Hill

[4] **Grainger, J. J. and Stevenson, W. D.** (1994). Power System Analysis. New York : McGraw Hill.

[5] **Nasar, S. A.** (1990). Electric Power Systems. New York : McGraw-Hill.

[6] **Güzelbeyoğlu, N.** (1997). Elektrik Makinalarında Aşırı Zorlanmalar. İstanbul : İTÜ.

[7] **Azevado, A. C., et al.** (2006). Investigation of Transformer Electromagnetic Forces Caused by External Faults Using FEM. Latin America : Transmission & Distribution Conference and Exposition.

[8] **Meng, Z. and Wang, Z.** (2004). The Analysis of Mechanical Strength of HV Winding Using Finite Element Method, Part 1 Calculation of Electromagnetic Forces. Bristol, UK : Universities Power Engineering Conference.

[9] **Meng , Z. and Wang , Z.** (2004). The Analysis of Mechanical Strength of HV Winding Using Finite Element Method, Part 2 Mechanical Stress and Deformation Analysis. Bristol, UK : Universities Power Engineering Conference.

[10] **Karsai, K., Kerenyi, D. and Kiss, L.** (1987). Large Power Transformers. Amsterdam : Elsevier.

[11] **Del Vecchio, R.M., et al., et al.** (2002). Transformer Design Principals with Applications to Core-Form Power Transformers. Boca Raton : CRC Press.

[12] **Çetiner, B. A.** (1993). Güç Transformatörlerinde Ayar Bobinlerinin Yerleştirilmesinin Sargı Kuvvetleri Bakımından incelenmesi. İstanbul: İTÜ, Master Thesis.

[13] **Dal, Murat, Kabasakal, S. and Kocabaş, D. A.**(2010). Trafolarda Kısa Devre Testi Simülasyonu ile Dayanım Analizi. İstanbul : Temsa Global A.Ş.

[14] **International standard IEC 60076-5.** (2006). Power Transformers - Part 5: Ability to Withstand Short Circuit.

CURRICULUM VITAE

Name Surname: Sadulah KAYA

EDUCATION:

B.Sc.: Middle East Technical University
Electrical and Electronics Engineering Department (2009)